

Rapamycin: Something Old, Something New, Sometimes Borrowed and Now Renewed

CM Hartford^{1,2} and MJ Ratain^{1,3,4}

The molecular target of rapamycin (mTOR) is central to a complex intracellular signaling pathway and is involved in diverse processes including cell growth and proliferation, angiogenesis, autophagy, and metabolism. Although sirolimus (rapamycin), the oldest inhibitor of mTOR, was discovered more than 30 years ago, renewed interest in this pathway is evident by the numerous rapalogs recently developed. These newer agents borrow from the structure of sirolimus and, although there are some pharmacokinetic differences, they appear to differ little in terms of pharmacodynamic effects and overall tolerability. Given the multitude of potential applications for this class of agents and the decrease in cost that can be expected upon the expiration of sirolimus patents, renewed focus on this agent is warranted.

Rapamycin (or sirolimus, the official generic name) is the prototypical inhibitor of the molecular target of rapamycin (mTOR). It was discovered more than 30 years ago as an antifungal agent and was approved in 1999 as an immunosuppressant for the prevention of renal allograft rejection. Over the years, with the elucidation of the complex intracellular signaling network in which mTOR participates and the realization of the multitude of potential therapeutic applications of interfering with this network, interest in agents that can inhibit mTOR has increased. There are currently three mTOR inhibitors in clinical trials, all either prodrugs or analogs of sirolimus, including temsirolimus, which was recently approved by the Food and Drug Administration (FDA) for the treatment of renal cancer. Although these newer agents (rapalogs) exhibit slightly different pharmacokinetic properties, they appear to differ little pharmacodynamically from sirolimus. This review will provide an overview of the mTOR pathway, discuss the pharmacokinetics and tolerability of the different mTOR inhibitors, and highlight the many potential clinical applications of these agents.

THE mTOR PATHWAY

The mTOR protein is a serine-threonine kinase that is central to a complex intracellular signaling pathway (Figure 1) and is involved in a number of important processes such as cell growth and proliferation, cellular metabolism, autophagy,

and angiogenesis. It responds to signals from the extracellular environment such as nutrient and growth factor supply, energy, and stress. Signaling through the pathway is promoted when there is an abundance of nutrients or energy and is downregulated in states of depletion and stress.¹

mTOR exists within the cell complexed to the proteins GβL and either raptor or rictor.² The mTOR/rictor protein complex is not responsive to inhibition by rapalogs and will not be discussed in detail except to mention its interaction with mTOR/raptor. The mTOR/GβL/raptor complex can be activated by various stimuli through different upstream molecules. Insulin (via the insulin receptor substrate-1) or other growth factors affect mTOR via the phosphoinositide-3 kinase (PI3K)/Akt pathway¹ (Figure 1). After stimulation, PI3K initiates a cascade that ultimately results in the phosphorylation and activation of Akt. Akt then acts via the tuberous sclerosis complex (TSC), consisting of the proteins TSC1 and TSC2, to exert its effect on mTOR. Phosphorylation of TSC2 by Akt inhibits TSC2, thereby releasing the inhibition that TSC2 otherwise exerts on mTOR via inhibition of Rheb, an activator of mTOR.¹

The energy status of the cell also affects mTOR signaling and acts via serine/threonine protein kinase 1 (LKB1) and AMP-activated kinase (AMPK). In states of energy depletion (increased AMP relative to ATP), LKB1 activates AMPK, which then activates TSC2, resulting in inhibition of the pathway.¹ Stress signals, for example, DNA damage and

¹Committee on Clinical Pharmacology and Pharmacogenomics, The University of Chicago, Chicago, Illinois, USA; ²Department of Pediatrics, The University of Chicago, Chicago, Illinois, USA; ³Department of Medicine, The University of Chicago, Chicago, Illinois, USA; ⁴Cancer Research Center, The University of Chicago, Chicago, Illinois, USA. Correspondence: MJ Ratain (mratain@medicine.bsd.uchicago.edu)

Published online 29 August 2007. doi:10.1038/sj.cpt.6100317

STATE OF THE ART

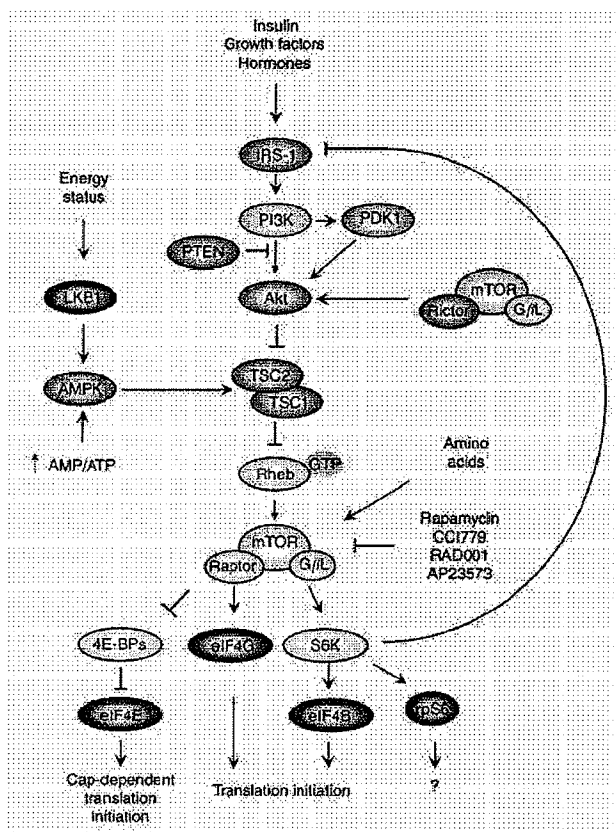


Figure 1 Schematic of the mTOR pathway. mTOR receives input from a number of upstream pathways, including PI3K/Akt, TSC1/TSC2, and AMPK, and acts through downstream effectors S6K and 4EBP1 to exert its effects.

hypoxia, also act via the TSC to cause an inhibition of mTOR signaling. The nutrient status of the cell, for example, amino-acid supply, influences the activity of mTOR. Although the mechanisms by which this occurs are less well characterized, it is known that the pathway is active when nutrients are readily available and downregulated in states of starvation.³

A number of other pathways can interact with the signaling described thus far. For example, phosphatase and tensin homolog (PTEN) is a tumor suppressor that counteracts the effects of PI3K by dephosphorylating phosphatidylinositol (3,4,5)-trisphosphate and therefore prevents activation of Akt.⁴ Neurofibromin 1 (NF1) inhibits Ras, which can activate the mTOR pathway via PI3K/Akt.⁵ Moreover, the mTOR/riCTOR complex can phosphorylate Akt, which therefore results in feedback and further signaling through the pathway.²

Downstream of mTOR are two main effectors, S6K1 and 4E-BP1, both of which control the translation of specific mRNAs and the synthesis of particular proteins. Phosphorylation of 4E-BP1 by mTOR ultimately results in the initiation of translation of certain mRNAs that have regulatory subunits in the 5'-untranslated terminal regions,

including those that are needed for cell cycle progression and are involved in cell cycle regulation.⁶ Phosphorylation and activation of S6K1 are also involved in cell growth and proliferation, possibly via translation of mRNAs that have a terminal 5'-oligopyrimidine tract such as those that encode ribosomal proteins and elongation factors. However, because translation of these latter genes was shown to be intact in S6K1^{-/-}/S6K2^{-/-} mice, other mechanisms are probably involved.⁷ Importantly, S6K1 also has an inhibitory feedback function on the pathway by phosphorylating and inhibiting insulin receptor substrate-1, thus reducing growth factor-stimulated signaling through PI3K/Akt/mTOR.⁸ It also phosphorylates and inactivates BCL2 antagonist of cell death (BAD), a proapoptotic molecule.⁶ The numerous proteins whose translation is regulated through mTOR and its downstream targets include cyclin D1, MYC avian myelocytomatosis viral oncogene homolog (c-MYC), and hypoxia-inducible factor-1 α (HIF-1 α).⁶

INHIBITORS OF THE mTOR PATHWAY

Mechanisms of action and mechanisms of resistance

Inhibitors of the mTOR pathway that are actively being studied include sirolimus, temsirolimus, everolimus, and AP23573 (now called deferolimus) (Figure 2). Sirolimus and the rapalogs exert their effects by the same mechanism. Each drug binds to the intracellular binding protein FK506-binding protein (FKBP12) to form a complex, which then binds to mTOR at the FKBP12-rapamycin binding domain, interfering with its ability to signal adequately to its downstream effectors. Exactly how the sirolimus-FKBP12 complex interrupts mTOR signaling is not known, but it may involve a destabilization of the interaction between mTOR and raptor.¹

Given the complexity of the mTOR pathway, there are many potential sites of resistance. Defects in the binding of sirolimus to FKBP12 because of mutations in FKBP12 and mutations in the FKBP12-rapamycin binding domain both confer resistance by interfering with the binding of the sirolimus-FKBP12 complex to mTOR.⁹ Other potential mechanisms of resistance include decreased levels of 4E-BP1 and mutations in S6K1.¹⁰ The complexity of the pathway and feedback loops within it may also contribute to resistance. For example, it is possible that inhibiting the negative feedback of S6K1 on insulin receptor substrate-1 may contribute to resistance to the antiproliferative effects of mTOR inhibition.⁹

Sirolimus. In the early 1970s, sirolimus, the first inhibitor of mTOR, was discovered as part of a screening program for new antifungal agents and was first named rapamycin because it was isolated from a soil sample from Rapa Nui.¹¹ Not long after, the inhibitory effect on the immune system was recognized in rats,¹² but it was not until the late 1980s¹³ and early 1990s¹⁴ that it was developed as an immunosuppressant. Both the antifungal and immunosuppressive activities are the result of the drug's ability to

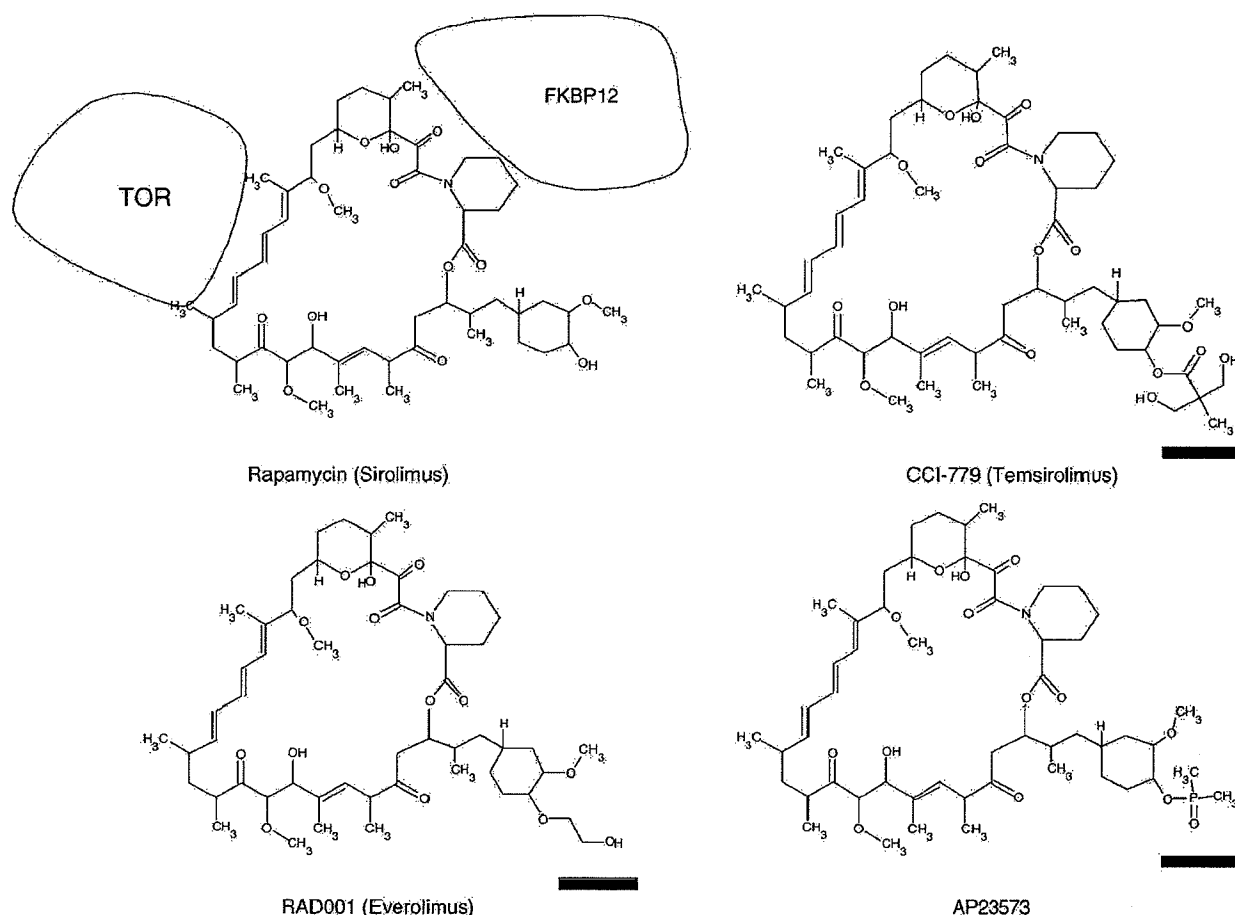


Figure 2 Inhibitors of the mammalian target of rapamycin (mTOR) pathway that are actively being investigated. The chemical structure of sirolimus and the newer analogues are similar. The bars indicate sites of structural differences among the agents.

interrupt the complex intracellular signaling cascade of the mTOR pathway, which is relatively conserved from yeasts to humans.¹⁵ As described, this ultimately causes a decrease in protein synthesis. In yeast and molds, the interruption of synthesis of proteins involved in cell cycle progression interferes with growth of the microorganisms.¹⁶ In T lymphocytes, this interferes with the ability of the cell to respond to cytokines and therefore blocks their proliferation and differentiation,¹⁷ leading to immunosuppression. As sirolimus had been used for the prevention of allograft rejection, most of the pharmacology data come from solid organ transplant patients.

Sirolimus is a macrocyclic lactone produced by *Streptomyces hygroscopicus*.¹⁸ It is poorly soluble in water and therefore can only be given orally. It is available in both liquid and tablet formulations. A study of stable renal allograft recipients in which patients were converted from liquid sirolimus to the tablet form demonstrated relative bioequivalent pharmacokinetics for the two formulations. Although the tablet formulation resulted in a lower maximum concentration (C_{max}), the area under the concentration-time curves (AUCs) of the two formulations were similar.¹⁹

Absorption of sirolimus is rapid with peak concentrations attained in about 2 h, but bioavailability is low ($\sim 15\%$)²⁰ and exhibits wide interpatient variability. This variability has been largely attributed to the effects of intestinal cytochrome P450 3A enzymes (CYP3A) and P-glycoprotein activity on sirolimus absorption.²¹ Studies on renal transplant patients have shown that the coadministration of cyclosporine affects the bioavailability of sirolimus and that when the drugs are administered concomitantly, both the C_{max} and the AUC of sirolimus are increased, possibly because of inhibition of CYP3A4 and P-glycoprotein by cyclosporine.²² The administration of a high-fat meal will also affect absorption. In a study of healthy volunteers, coadministration of sirolimus with a high-fat meal resulted in a slower absorption but a 35% increase in AUC.²³

The volume of distribution of sirolimus is large (~ 121 kg), indicating wide distribution into tissues and necessitating, in many instances, a loading dose. Most of the drug partitions into red blood cells ($\sim 95\%$), with small amounts in lymphocytes and granulocytes ($\sim 1\%$ each).²⁴ Of the 3% in plasma, only 2.5% is free and the remainder is protein-bound.²⁴

The metabolism of sirolimus is mainly via hepatic CYP3A enzymes. In a study of 18 adults with mild to moderate hepatic impairment, AUC and half-life of sirolimus were significantly increased and weight-normalized apparent oral clearance was significantly decreased, as compared with healthy controls,²⁵ suggesting that dose adjustments may be needed for patients with hepatic impairment. Sirolimus has multiple metabolites, all with low immunosuppressive activity (<10% relative to sirolimus).²⁶ The excretion is primarily fecal. The clearance is widely variable (1.45–6.93 ml/min/kg) and the half-life is long (~62 h),²⁰ allowing for once-daily dosing.

The interaction of sirolimus with CYP3A4 and P-glycoprotein not only leads to wide interpatient variability in absorption and metabolism but also to the potential for a number of drug interactions. Commonly encountered inhibitors of CYP3A4 and P-glycoprotein include ketoconazole, cyclosporine, erythromycin, and ritonavir, along with grapefruit juice; inducers of CYP3A4 include dexamethasone, phenytoin, carbamazepine, rifampin, and phenobarbital, to name a few. These medications should be used cautiously and avoided if possible in patients treated with sirolimus.

When used as an immunosuppressant for the prevention of solid organ graft rejection, therapeutic drug monitoring has been an important issue. A study of 150 renal transplant patients showed a correlation between trough drug levels (which correlate well with sirolimus AUC) and both incidence of adverse side effects (for levels >15 ng/ml) and acute graft rejection (for levels <5 ng/ml).²⁷ One approach that has been recommended is to monitor all patients during the initial phase of treatment (for ~2 months) and thereafter based on individual patient characteristics.²⁸

Rapalogs. Temsirolimus, everolimus, and deferolimus (Figure 2) are all structurally similar to sirolimus, differing mainly at a single position of the lactone ring (C-40) unrelated to both the mTOR- and FKBP12-binding sites. Temsirolimus is a water-soluble dihydroxymethyl propionic acid ester prodrug of sirolimus. Both intravenous and oral formulations are available, although recent development has focused on the intravenous formulation. To date, temsirolimus has been mainly developed as an anticancer agent, and it was approved by the FDA on 30 May 2007 for the treatment of advanced renal cell carcinoma. Everolimus is an oral 40-O-(2-hydroxyethyl) derivative (not prodrug) of sirolimus approved in Europe as an immunosuppressant for the prevention of cardiac and renal allograft rejection in adults.²⁹ More recently, it has been studied as an anticancer agent. Deferolimus is the newest addition to the rapalogs. It contains a phosphine oxide substitute on the lactone ring and is available in both oral and intravenous formulations. It is currently being investigated for the treatment of a number of different malignancies.

As mentioned, sirolimus and the rapalogs inhibit mTOR by forming a complex with FKBP12, which then binds to mTOR. Few data are available regarding differences in the

ability of the drugs to inhibit mTOR. One study showed that the binding of everolimus to FKBP12 was approximately threefold weaker than that of sirolimus *in vitro*.³⁰ However, further *in vivo* studies on rats showed similar efficacy of the two agents in terms of immunosuppressive activity. The mTOR inhibitors are very specific in their action, and there is no evidence to date of any effects other than those on mTOR. All are known to result in a decrease in the phosphorylation of the downstream effectors 4E-BP1 and S6K1^{31–34} and the degree of this effect is being studied as a potential biomarker of mTOR inhibition.

An often stated reason for the development of new mTOR inhibitors is to improve the pharmacokinetic properties of sirolimus, mainly the poor bioavailability and insolubility in water. The chemical modifications of temsirolimus and deferolimus have resulted in water-soluble formulations that are currently being studied as intravenous agents. Few data are available regarding the oral formulations of these rapalogs and, to date, the main oral alternative to sirolimus is everolimus. Although everolimus exhibits greater polarity than sirolimus, the bioavailability is only slightly improved and is still relatively low (~16%).³⁵ Similar to sirolimus, CYP3A4 and P-glycoprotein affect its absorption and contribute to wide interpatient variability.³⁶

The rapalogs share many characteristics with sirolimus, including extensive partitioning into red blood cells,^{36,37} metabolism by hepatic CYP3A enzymes,^{38,39} and primarily fecal excretion.³⁵ In a study of patients with liver cirrhosis, the clearance of everolimus was reduced by 53% and the half-life prolonged 84%, showing the need for dose reductions in patients with liver impairment.⁴⁰ Although similar studies of temsirolimus have not been published, given the extensive hepatic metabolism, it is possible that this agent may also require dose adjustment in patients with liver dysfunction. As the rapalogs are substrates of CYP3A4 and P-glycoprotein, potential drug interactions are also a concern, as with sirolimus. There are differences in the half-lives, potentially affecting the optimal dosing schedules. The half-life of everolimus in stable renal transplant patients was 24–35 h⁴¹ and 13–25^{42,43} and 45–74 h,³⁷ respectively, for the intravenous formulations of temsirolimus and deferolimus.

Temsirolimus is the only rapalog that is a prodrug. It quickly undergoes hydrolysis to sirolimus after intravenous administration. Sirolimus can be seen as early as 15 min after the start of temsirolimus infusion, reaches peak concentration at 0.5–2.0 h, and then decreases monoexponentially.⁴³ After a dose of temsirolimus, the exposure to sirolimus exceeds that of parent drug because of the differences in half-lives, with the mean sirolimus/temsirolimus ratio being 2.5–3.5.⁴³ Although temsirolimus exhibits inhibitory activity against mTOR, most of its clinical effects are probably due to the sirolimus metabolite.^{44,45}

Tolerability of the mTOR inhibitors

The four mTOR inhibitors exhibit remarkably similar side effect profiles and are in general well tolerated by patients,

Table 1 Multiple applications of mTOR inhibitors that have been studied, both clinically and preclinically, along with the rationale for possible efficacy of mTOR inhibition

Application	Rationale	Comments	Clinical data	Preclinical data
<i>Immune</i>				
Graft rejection GVHD Autoimmune diseases ALPS Asthma	Inhibition of proliferation of T cells in response to growth-promoting cytokines (IL-2) Inhibition of proliferation of B cells and mast cells Suppression of B-cell immunoglobulin production in response to certain stimuli	Effects of mTOR inhibitors on T-cell subsets and function: Increase in the suppressor function of CD4+ T cells Thymic atrophy and a reduction in CD4+CD8+ thymocytes secondary to increased apoptosis without affecting total numbers of T and B cells in the periphery An increase in the percent of CD4+CD25+ regulatory T cells An increase in the numbers of alloreactive CD103+CD8+ regulatory T cells	Refs. 51-61	Refs. 17, 62-71
<i>Cancer</i>				
Malignant tumors Benign hamartomas Radiation and chemosensitization	Antiproliferative effect by inhibiting cell cycle progression and causing G ₁ arrest Proapoptotic effect by interfering with phosphorylation of BAD Antiangiogenic effect by interfering with HIF-1 α Many proteins involved in hamartoma syndromes are linked to the mTOR pathway Radiation can induce signaling of Akt/mTOR, which can be attenuated by mTOR inhibition	Many different tumor types have shown responsiveness to mTOR inhibition, including both solid tumors and hematologic malignancies At doses used for anticancer treatment, mTOR inhibitors do not appear to be immunosuppressive TSC1/TSC2 (tuberous sclerosis), PTEN (Cowden disease), LKB1 (Peutz-Jeghers syndrome), NF1 (neurofibromatosis) are hamartoma syndromes linked to the mTOR pathway Other potential applications of the antiangiogenic effect of mTOR inhibitors include diseases characterized by neovascularization, such as endometriosis and keratitis	Refs. 72-75	Refs. 5, 67, 76-89
<i>Benign diseases characterized by abnormal proliferation</i>				
Cardiac stents Hypertrophic myocarditis Pulmonary fibrosis Hepatic fibrosis ADPKD	By blocking progression through the cell cycle and causing G ₁ arrest, mTOR inhibitors have an antiproliferative effect that may be beneficial for a number of different benign diseases	Sirolimus-eluting stents were approved in 2003 for angioplasty to open clogged coronary arteries	Refs. 90-92	Refs. 93-98
<i>Neurodegenerative disorders</i>				
Huntington disease	Huntington disease is characterized by accumulation of intraneuronal proteins that interfere with cellular processes. Increased autophagy, through inhibition of mTOR, may increase the degradation of the intracellular proteins that characterize Huntington disease			Refs. 99, 100
<i>Infectious diseases</i>				
Fungal infections HIV	The mTOR pathway is relatively conserved from yeasts to humans. Blocking the pathway in yeasts and fungi interferes with their growth and proliferation Infection with HIV-1 requires expression of the viral coreceptor CCR5 on the cell surface. In T cells, this expression depends on signaling through IL-2, which is blocked by mTOR inhibition	Early studies demonstrated potent activity against <i>Candida albicans</i> and <i>Aspergillus</i> , among other species. However, because of the immunosuppressive effects, these are not typically used for treatment of fungal infections		Refs. 16, 18, 101, 102
<i>Metabolic disorders</i>				
Type II diabetes Obesity	Via intracellular connection with the insulin receptor/IRS-1/PI3K/Akt pathway and its role in cellular response to nutrients, mTOR may be important in the development of insulin resistance and obesity			Refs. 103, 104

ADPKD, autosomal dominant polycystic kidney disease; ALPS, autoimmune lymphoproliferative syndrome; CCR5, CC chemokine receptor 5; GVHD, graft-versus-host disease; HIV, human immunodeficiency virus; IL-2, interleukin-2; IRS-1, insulin receptor substrate-1; mTOR, molecular target of rapamycin; PI3K, phosphoinositide-3 kinase; TSC, tuberous sclerosis complex.

adding to the attractiveness of this class of drugs. Classically described adverse effects include fatigue, rash, mucositis, anorexia, and gastrointestinal effects such as diarrhea and nausea; hematologic effects include thrombocytopenia, leukopenia, and anemia; and metabolic effects include hyperlipidemia, hyperglycemia, and hypercholesterolemia.^{20,33,43,46} In most cases, the adverse effects can be managed with dose reductions or, in the case of metabolic disturbances, with the addition of insulin or a cholesterol-lowering medication.

A rarer and potentially serious side effect that has been noted with these agents is interstitial pneumonitis.⁴⁷ In a series of 24 renal transplant patients who developed pneumonitis associated with sirolimus, symptoms included cough, fatigue, and fever in the majority of patients, and eight patients also developed dyspnea.⁴⁸ One patient was asymptomatic. Imaging by computed tomography revealed patchy bilateral infiltrates to be the most common finding (19 patients). Sirolimus was discontinued in all patients and all recovered completely within 6 months. Similar reports after treatment with temsirolimus exist⁴⁹ and pneumonitis is listed as an uncommon side effect of everolimus (Certican, prescribing information).

The first approved application of mTOR inhibitors was as an immunosuppressant. The effects on the immune system may be of some concern when these agents are used for other purposes and especially when administered to patients with cancer. However, despite the ability to block proliferation of certain cells of the immune system, there has not been a significant number of infectious complications with the doses and schedules used in clinical oncology trials. Most published trials have not reported specific analyses of T-cell subsets or function, but a phase I study of temsirolimus mentioned that lymphocyte cell-surface phenotype analysis and mitogen proliferation assays did not show any trend toward immunosuppression.⁴²

Applications of mTOR inhibitors

Because of mTOR's complex effects on protein synthesis and cell cycle progression, interfering with its signaling can lead to a number of potentially therapeutic outcomes. For example, by interfering with the translation of proteins involved in cell cycle progression, inhibition of mTOR results in arrest in G₁ of the cell cycle and an antiproliferative effect that may be beneficial for the treatment of cancer and a number of benign diseases associated with abnormal proliferation. Immunosuppression can occur by interfering with protein synthesis within certain cells of the immune system, such as T cells. Interfering with the translation of HIF-1 α has an antiangiogenic effect, and inhibiting the phosphorylation of BAD by S6K1 may promote apoptosis. Another effect of mTOR inhibition is to promote autophagy, although the exact mechanism of this remains unknown.⁵⁰ These multiple and diverse effects may potentially result in a number of important therapeutic applications for the treatment of a wide range of diseases. The various diseases

for which inhibition of the mTOR pathway has been studied, both clinically and preclinically, along with the rationale for why inhibiting the pathway may be efficacious, are listed in Table 1.

CONCLUSION

The mTOR pathway plays a central role in a number of important intracellular processes. Blocking the pathway with sirolimus or a rapalog has implications for the treatment of many diverse diseases. Although many studies are currently underway and more data will be collected, the newer mTOR inhibitors appear to be potentially interchangeable with sirolimus (if administered at a comparable dose and schedule). Wide interpatient variability in pharmacokinetics, metabolism by CYP3A4, and therefore the potential for numerous drug interactions, poor bioavailability of the oral agents, and generally good tolerability are characteristics of this class of drugs. There is no convincing evidence thus far to suggest that the newer agents offer a large advantage to sirolimus. Given the limited patent exclusivity and the decrease in cost that can be expected upon expiration of the sirolimus patents, perhaps more focus should be given to the oldest agent so that it can be effectively applied for the multitude of new potential uses being discovered, rather than continuing to borrow from it for the production of more new inhibitors of mTOR.

ACKNOWLEDGMENTS

Dr Hartford was supported by T32 GM007019 from the NIH.

CONFLICT OF INTEREST

The authors declared no conflict of interest.

© 2007 American Society for Clinical Pharmacology and Therapeutics

1. Wullschlegel, S., Loewith, R. & Hall, M.N. TOR signaling in growth and metabolism. *Cell* **124**, 471-484 (2006).
2. Sarbassov, D.D., Ali, S.M. & Sabatini, D.M. Growing roles for the mTOR pathway. *Curr. Opin. Cell. Biol.* **17**, 596-603 (2005).
3. Avruch, J., Lin, Y., Long, X., Murthy, S. & Ortiz-Vega, S. Recent advances in the regulation of the TOR pathway by insulin and nutrients. *Curr. Opin. Clin. Nutr. Metab. Care* **8**, 67-72 (2005).
4. Rowinsky, E.K. Targeting the molecular target of rapamycin (mTOR). *Curr. Opin. Oncol.* **16**, 564-575 (2004).
5. Johannessen, C.M. et al. The NF1 tumor suppressor critically regulates TSC2 and mTOR. *Proc. Natl. Acad. Sci. USA* **102**, 8573-8578 (2005).
6. Faivre, S., Kroemer, G. & Raymond, E. Current development of mTOR inhibitors as anticancer agents. *Nat. Rev. Drug Discov.* **5**, 671-688 (2006).
7. Pende, M. et al. S6K1(-/-)/S6K2(-/-) mice exhibit perinatal lethality and rapamycin-sensitive 5'-terminal oligopyrimidine mRNA translation and reveal a mitogen-activated protein kinase-dependent S6 kinase pathway. *Mol. Cell. Biol.* **24**, 3112-3124 (2004).
8. Petroulakis, E., Mamane, Y., Le Bacquer, O., Shahbazian, D. & Sonenberg, N. mTOR signaling: implications for cancer and anticancer therapy. *Br. J. Cancer* **94**, 195-199 (2006).
9. Kurmasheva, R.T., Huang, S. & Houghton, P.J. Predicted mechanisms of resistance to mTOR inhibitors. *Br. J. Cancer* **95**, 955-960 (2006).
10. Huang, S., Bjornsti, M.A. & Houghton, P.J. Rapamycin: mechanism of action and cellular resistance. *Cancer Biol. Ther.* **2**, 222-232 (2003).
11. Sehgal, S.N., Baker, H. & Vezina, C. Rapamycin (AY-22,989), a new antifungal antibiotic. II. Fermentation, isolation and characterization. *J. Antibiot. (Tokyo)* **28**, 727-732 (1975).
12. Martel, R.R., Klicius, J. & Galet, S. Inhibition of the immune response by rapamycin, a new antifungal antibiotic. *Can. J. Physiol. Pharmacol.* **55**, 48-51 (1977).

13. Calne, R.Y. *et al.* Rapamycin for immunosuppression in organ allografting. *Lancet* **2**, 227 (1989).
14. Kahan, B.D., Chang, J.Y. & Sehgal, S.N. Preclinical evaluation of a new potent immunosuppressive agent, rapamycin. *Transplantation* **52**, 185-191 (1991).
15. Cardenas, M.E. *et al.* Antifungal activities of antineoplastic agents: *Saccharomyces cerevisiae* as a model system to study drug action. *Clin. Microbiol. Rev.* **12**, 583-611 (1999).
16. Singh, N. & Heitman, J. Antifungal attributes of immunosuppressive agents: new paradigms in management and elucidating the pathophysiologic basis of opportunistic mycoses in organ transplant recipients. *Transplantation* **77**, 795-800 (2004).
17. Dumont, F.J. & Su, Q. Mechanism of action of the immunosuppressant rapamycin. *Life Sci.* **58**, 373-395 (1996).
18. Singh, K., Sun, S. & Vezina, C. Rapamycin (AY-22,989), a new antifungal antibiotic. IV. Mechanism of action. *J. Antibiot. (Tokyo)* **32**, 630-645 (1979).
19. Kelly, P.A., Napoli, K. & Kahan, B.D. Conversion from liquid to solid rapamycin formulations in stable renal allograft transplant recipients. *Biopharm. Drug Dispos.* **20**, 249-253 (1999).
20. Napoli, K.L. & Taylor, P.J. From beach to bedside: history of the development of sirolimus. *Ther. Drug Monit.* **23**, 559-586 (2001).
21. Mahalati, K. & Kahan, B.D. Clinical pharmacokinetics of sirolimus. *Clin. Pharmacokinet.* **40**, 573-585 (2001).
22. Kaplan, B., Meier-Kriesche, H.U., Napoli, K.L., & Kahan, B.D. The effects of relative timing of sirolimus and cyclosporine microemulsion formulation coadministration on the pharmacokinetics of each agent. *Clin. Pharmacol. Ther.* **63**, 48-53 (1998).
23. Zimmerman, J.J., Ferron, G.M., Lim, H.K. & Parker, V. The effect of a high-fat meal on the oral bioavailability of the immunosuppressant sirolimus (rapamycin). *J. Clin. Pharmacol.* **39**, 1155-1161 (1999).
24. Yatscoff, R., LeGat, D., Keenan, R. & Chackowsky, P. Blood distribution of rapamycin. *Transplantation* **56**, 1202-1206 (1993).
25. Zimmerman, J.J. *et al.* Pharmacokinetics of sirolimus (rapamycin) in subjects with mild to moderate hepatic impairment. *J. Clin. Pharmacol.* **45**, 1368-1372 (2005).
26. Trepanier, D.J., Gallant, H., Legatt, D.F. & Yatscoff, R.W. Rapamycin: distribution, pharmacokinetics and therapeutic range investigations: an update. *Clin. Biochem.* **31**, 345-351 (1998).
27. Kahan, B.D. *et al.* Therapeutic drug monitoring of sirolimus: correlations with efficacy and toxicity. *Clin. Transplant.* **14**, 97-109 (2000).
28. Stenton, S.B., Partovi, N. & Ensom, M.H. Sirolimus: the evidence for clinical pharmacokinetic monitoring. *Clin. Pharmacokinet.* **44**, 769-786 (2005).
29. Chapman, T.M. & Perry, C.M. Everolimus. *Drugs* **64**, 861-872 (2004); discussion 864-873.
30. Schuler, W. *et al.* SDZ RAD, a new rapamycin derivative: pharmacological properties *in vitro* and *in vivo*. *Transplantation* **64**, 36-42 (1997).
31. Dudkin, L. *et al.* Biochemical correlates of mTOR inhibition by the rapamycin ester CCI-779 and tumor growth inhibition. *Clin. Cancer Res.* **7**, 1758-1764 (2001).
32. Galanis, E. *et al.* Phase II trial of temsirolimus (CCI-779) in recurrent glioblastoma multiforme: a North Central Cancer Treatment Group Study. *J. Clin. Oncol.* **23**, 5294-5304 (2005).
33. Yee, K.W. *et al.* Phase I/II study of the mammalian target of rapamycin inhibitor everolimus (RAD001) in patients with relapsed or refractory hematologic malignancies. *Clin. Cancer Res.* **12**, 5165-5173 (2006).
34. Mita, M.M. *et al.* Phase I, pharmacokinetic (PK), and pharmacodynamic (PD) study of AP23573, an mTOR inhibitor, administered IV daily X 5 every other week in patients (pts) with refractory or advanced malignancies. *J. Clin. Oncol. (Meeting Abstracts)* **22**, 3076 (2004).
35. Kirchner, G.J., Meier-Wiedenbach, I. & Manns, M.P. Clinical pharmacokinetics of everolimus. *Clin. Pharmacokinet.* **43**, 83-95 (2004).
36. Kovarik, J.M. *et al.* Longitudinal assessment of everolimus in *de novo* renal transplant recipients over the first post-transplant year: pharmacokinetics, exposure-response relationships, and influence on cyclosporine. *Clin. Pharmacol. Ther.* **69**, 48-56 (2001).
37. Desai, A.A. *et al.* Development of a pharmacokinetic (PK) model and assessment of patient (pt) covariate effects on dose-dependent PK following different dosing schedules in two phase I trials of AP23573 (AP), a mTOR inhibitor. *J. Clin. Oncol. (Meeting Abstracts)* **23**, 3043 (2005).
38. Cai, P., Tsao, R. & Ruppen, M.E. *In Vitro* Metabolic Study Of Temsirolimus: Preparation, Isolation, And Identification Of The Metabolites. *Drug Metab Dispos.* **35**, 1554-1563 (2007).
39. Jacobsen, W. *et al.* Comparison of the *in vitro* metabolism of the macrolide immunosuppressants sirolimus and RAD. *Transplant. Proc.* **33**, 514-515 (2001).
40. Kovarik, J.M. *et al.* Influence of hepatic impairment on everolimus pharmacokinetics: implications for dose adjustment. *Clin. Pharmacol. Ther.* **70**, 425-430 (2001).
41. Neumayer, H.H. *et al.* Entry-into-human study with the novel immunosuppressant SDZ RAD in stable renal transplant recipients. *Br. J. Clin. Pharmacol.* **48**, 694-703 (1999).
42. Hidalgo, M. *et al.* A phase I and pharmacokinetic study of temsirolimus (CCI-779) administered intravenously daily for 5 days every 2 weeks to patients with advanced cancer. *Clin. Cancer Res.* **12**, 5755-5763 (2006).
43. Raymond, E. *et al.* Safety and pharmacokinetics of escalated doses of weekly intravenous infusion of CCI-779, a novel mTOR inhibitor, in patients with cancer. *J. Clin. Oncol.* **22**, 2336-2347 (2004).
44. Zeng, Z. *et al.* Rapamycin derivatives reduce mTORC2 signaling and inhibit AKT activation in AML. *Blood* **109**, 3509-3512 (2007).
45. Del Bufalo, D. *et al.* Antiangiogenic potential of the mammalian target of rapamycin inhibitor temsirolimus. *Cancer Res.* **66**, 5549-5554 (2006).
46. Chawla, S.P. *et al.* Updated results of a phase II trial of AP23573, a novel mTOR inhibitor, in patients (pts) with advanced soft tissue or bone sarcomas. *J. Clin. Oncol. (Meeting Abstracts)* **24**, 9505 (2006).
47. Buhaescu, I., Izzedine, H. & Covic, A. Sirolimus—challenging current perspectives. *Ther. Drug Monit.* **28**, 577-584 (2006).
48. Champion, L. *et al.* Brief communication: sirolimus-associated pneumonitis: 24 cases in renal transplant recipients. *Ann. Intern. Med.* **144**, 505-509 (2006).
49. Duran, I. *et al.* Characterisation of the lung toxicity of the cell cycle inhibitor temsirolimus. *Eur. J. Cancer* **42**, 1875-1880 (2006).
50. Rubinsztein, D.C., Gestwicki, J.E., Murphy, L.O. & Klionsky, D.J. Potential therapeutic applications of autophagy. *Nat. Rev. Drug Discov.* **6**, 304-312 (2007).
51. Levy, G. *et al.* Safety, tolerability, and efficacy of everolimus in *de novo* liver transplant recipients: 12- and 36-month results. *Liver Transpl.* **12**, 1640-1648 (2006).
52. Snell, G.I. *et al.* Everolimus versus azathioprine in maintenance lung transplant recipients: an international, randomized, double-blind clinical trial. *Am. J. Transplant.* **6**, 169-177 (2006).
53. Keogh, A. *et al.* Sirolimus in *de novo* heart transplant recipients reduces acute rejection and prevents coronary artery disease at 2 years: a randomized clinical trial. *Circulation* **110**, 2694-2700 (2004).
54. Kerkar, N. *et al.* Rapamycin successfully treats post-transplant autoimmune hepatitis. *Am. J. Transplant.* **5**, 1085-1089 (2005).
55. Cutler, C. & Antin, J.H. Sirolimus for GVHD prophylaxis in allogeneic stem cell transplantation. *Bone Marrow Transplant.* **34**, 471-476 (2004).
56. Benito, A.I. *et al.* Sirolimus (rapamycin) for the treatment of steroid-refractory acute graft-versus-host disease. *Transplantation* **72**, 1924-1929 (2001).
57. Couriel, D.R. *et al.* Sirolimus in combination with tacrolimus and corticosteroids for the treatment of resistant chronic graft-versus-host disease. *Br. J. Haematol.* **130**, 409-417 (2005).
58. Fernandez, D., Bonilla, E., Mirza, N., Niland, B. & Perl, A. Rapamycin reduces disease activity and normalizes T cell activation-induced calcium fluxing in patients with systemic lupus erythematosus. *Arthritis Rheum.* **54**, 2983-2988 (2006).
59. Nadiminti, U. & Arbisser, J.L. Rapamycin (sirolimus) as a steroid-sparing agent in dermatomyositis. *J. Am. Acad. Dermatol.* **52**, 17-19 (2005).
60. Valentini, R.P. *et al.* Sirolimus rescue for tacrolimus-associated post-transplant autoimmune hemolytic anemia. *Pediatr. Transplant.* **10**, 358-361 (2006).
61. Foronczewicz, B., Mucha, K., Paczek, L., Chmura, A. & Rowinski, W. Efficacy of rapamycin in patient with juvenile rheumatoid arthritis. *Transpl. Int.* **18**, 366-368 (2005).
62. Majewski, M. *et al.* The immunosuppressive macrolide RAD inhibits growth of human Epstein-Barr virus-transformed B lymphocytes

- in vitro* and *in vivo*: a potential approach to prevention and treatment of posttransplant lymphoproliferative disorders. *Proc. Natl. Acad. Sci. USA* **97**, 4285–4290 (2000).
63. Baeder, W.L., Sredy, J., Sehgal, S.N., Chang, J.Y. & Adams, L.M. Rapamycin prevents the onset of insulin-dependent diabetes mellitus (IDDM) in NOD mice. *Clin. Exp. Immunol.* **89**, 174–178 (1992).
 64. Ikeda, E., Hikita, N., Eto, K. & Mochizuki, M. Tacrolimus-rapamycin combination therapy for experimental autoimmune uveoretinitis. *Jpn. J. Ophthalmol.* **41**, 396–402 (1997).
 65. Martin, D.F., DeBarge, L.R., Nussenblatt, R.B., Chan, C.C. & Roberge, F.G. Synergistic effect of rapamycin and cyclosporin A in the treatment of experimental autoimmune uveoretinitis. *J. Immunol.* **154**, 922–927 (1995).
 66. Teachey, D.T. *et al.* Rapamycin improves lymphoproliferative disease in murine autoimmune lymphoproliferative syndrome (ALPS). *Blood* **108**, 1965–1971 (2006).
 67. Brown, V.I. *et al.* Rapamycin is active against B-precursor leukemia *in vitro* and *in vivo*, an effect that is modulated by IL-7-mediated signaling. *Proc. Natl. Acad. Sci. USA* **100**, 15113–15118 (2003).
 68. Haczu, A. *et al.* The effect of dexamethasone, cyclosporine, and rapamycin on T-lymphocyte proliferation *in vitro*: comparison of cells from patients with glucocorticoid-sensitive and glucocorticoid-resistant chronic asthma. *J. Allergy Clin. Immunol.* **93**, 510–519 (1994).
 69. Valmori, D. *et al.* Rapamycin-mediated enrichment of T cells with regulatory activity in stimulated CD4⁺ T cell cultures is not due to the selective expansion of naturally occurring regulatory T cells but to the induction of regulatory functions in conventional CD4⁺ T cells. *J. Immunol.* **177**, 944–949 (2006).
 70. Uss, E., Yong, S.L., Hooibrink, B., van Lier, R.A. & ten Berge, I.J. Rapamycin enhances the number of alloantigen-induced human CD103⁺CD8⁺ regulatory T cells *in vitro*. *Transplantation* **83**, 1098–1106 (2007).
 71. Tian, L., Lu, L., Yuan, Z., Lamb, J.R. & Tam, P.K. Acceleration of apoptosis in CD4⁺CD8⁺ thymocytes by rapamycin accompanied by increased CD4⁺CD25⁺ T cells in the periphery. *Transplantation* **77**, 183–189 (2004).
 72. Chan, S. *et al.* Phase II study of temsirolimus (CCI-779), a novel inhibitor of mTOR, in heavily pretreated patients with locally advanced or metastatic breast cancer. *J. Clin. Oncol.* **23**, 5314–5322 (2005).
 73. Atkins, M.B. *et al.* Randomized phase II study of multiple dose levels of CCI-779, a novel mammalian target of rapamycin kinase inhibitor, in patients with advanced refractory renal cell carcinoma. *J. Clin. Oncol.* **22**, 909–918 (2004).
 74. Hudes, G. *et al.* A phase 3, randomized, 3-arm study of temsirolimus (TEMSR) or interferon-alpha (IFN) or the combination of TEMSR+IFN in the treatment of first-line, poor-risk patients with advanced renal cell carcinoma (adv RCC). *J. Clin. Oncol. (Meeting Abstracts)* **24**, LBA4 (2006).
 75. Hudes, G. *et al.* Temsirolimus, interferon alfa, or both for advanced renal-cell carcinoma. *N. Engl. J. Med.* **356**, 2271–2281 (2007).
 76. Hosoi, H. *et al.* Rapamycin causes poorly reversible inhibition of mTOR and induces p53-independent apoptosis in human rhabdomyosarcoma cells. *Cancer Res.* **59**, 886–894 (1999).
 77. Mateo-Lozano, S., Tirado, O.M. & Notario, V. Rapamycin induces the fusion-type independent downregulation of the EWS/FLI-1 proteins and inhibits Ewing's sarcoma cell proliferation. *Oncogene* **22**, 9282–9287 (2003).
 78. Wan, X., Mendoza, A., Khanna, C. & Helman, L.J. Rapamycin inhibits ezrin-mediated metastatic behavior in a murine model of osteosarcoma. *Cancer Res.* **65**, 2406–2411 (2005).
 79. Xu, Q., Thompson, J.E. & Carroll, M. mTOR regulates cell survival after etoposide treatment in primary AML cells. *Blood* **106**, 4261–4268 (2005).
 80. Decker, T. *et al.* Rapamycin-induced G₁ arrest in cycling B-CLL cells is associated with reduced expression of cyclin D3, cyclin E, cyclin A, and survivin. *Blood* **101**, 278–285 (2003).
 81. Haritunians, T. *et al.* Antiproliferative activity of RAD001 (everolimus) as a single agent and combined with other agents in mantle cell lymphoma. *Leukemia* **21**, 333–339 (2007).
 82. Albert, J.M., Kim, K.W., Cao, C. & Lu, B. Targeting the Akt/mammalian target of rapamycin pathway for radiosensitization of breast cancer. *Mol. Cancer Ther.* **5**, 1183–1189 (2006).
 83. Beuvink, I. *et al.* The mTOR inhibitor RAD001 sensitizes tumor cells to DNA-damaged induced apoptosis through inhibition of p21 translation. *Cell* **120**, 747–759 (2005).
 84. Lee, L. *et al.* Efficacy of a rapamycin analog (CCI-779) and IFN-gamma in tuberous sclerosis mouse models. *Genes Chromosomes Cancer* **42**, 213–227 (2005).
 85. Laschke, M.W. *et al.* Rapamycin induces regression of endometriotic lesions by inhibiting neovascularization and cell proliferation. *Br. J. Pharmacol.* **149**, 137–144 (2006).
 86. Kwon, Y.S., Hong, H.S., Kim, J.C., Shin, J.S. & Son, Y. Inhibitory effect of rapamycin on corneal neovascularization *in vitro* and *in vivo*. *Invest. Ophthalmol. Vis. Sci.* **46**, 454–460 (2005).
 87. Recher, C. *et al.* Antileukemic activity of rapamycin in acute myeloid leukemia. *Blood* **105**, 2527–2534 (2005).
 88. Platzbecker, U. *et al.* Activity of sirolimus in patients with myelodysplastic syndrome—results of a pilot study. *Br. J. Haematol.* **128**, 625–630 (2005).
 89. Franz, D.N. *et al.* Rapamycin causes regression of astrocytomas in tuberous sclerosis complex. *Ann. Neurol.* **59**, 490–498 (2006).
 90. Hausleiter, J. *et al.* Randomized, double-blind, placebo-controlled trial of oral sirolimus for restenosis prevention in patients with in-stent restenosis: the Oral Sirolimus to Inhibit Recurrent In-stent Stenosis (OSIRIS) trial. *Circulation* **110**, 790–795 (2004).
 91. Moses, J.W. *et al.* Sirolimus-eluting stents versus standard stents in patients with stenosis in a native coronary artery. *N. Engl. J. Med.* **349**, 1315–1323 (2003).
 92. Shillingford, J.M. *et al.* The mTOR pathway is regulated by polycystin-1, and its inhibition reverses renal cystogenesis in polycystic kidney disease. *Proc. Natl. Acad. Sci. USA* **103**, 5466–5471 (2006).
 93. Shioi, T. *et al.* Rapamycin attenuates load-induced cardiac hypertrophy in mice. *Circulation* **107**, 1664–1670 (2003).
 94. Maeda, K. *et al.* Rapamycin ameliorates experimental autoimmune myocarditis. *Int. Heart J.* **46**, 513–530 (2005).
 95. Shegogue, D. & Trojanowska, M. Mammalian target of rapamycin positively regulates collagen type I production via a phosphatidylinositol 3-kinase-independent pathway. *J. Biol. Chem.* **279**, 23166–23175 (2004).
 96. Simler, N.R. *et al.* The rapamycin analogue SDZ RAD attenuates bleomycin-induced pulmonary fibrosis in rats. *Eur. Respir. J.* **19**, 1124–1127 (2002).
 97. Biecker, E. *et al.* Long-term treatment of bile duct-ligated rats with rapamycin (sirolimus) significantly attenuates liver fibrosis: analysis of the underlying mechanisms. *J. Pharmacol. Exp. Ther.* **313**, 952–961 (2005).
 98. Bonegio, R.G. *et al.* Rapamycin ameliorates proteinuria-associated tubulointerstitial inflammation and fibrosis in experimental membranous nephropathy. *J. Am. Soc. Nephrol.* **16**, 2063–2072 (2005).
 99. Ravikumar, B., Duden, R. & Rubinsztein, D.C. Aggregate-prone proteins with polyglutamine and polyalanine expansions are degraded by autophagy. *Hum. Mol. Genet.* **11**, 1107–1117 (2002).
 100. Ravikumar, B. *et al.* Inhibition of mTOR induces autophagy and reduces toxicity of polyglutamine expansions in fly and mouse models of Huntington disease. *Nat. Genet.* **36**, 585–595 (2004).
 101. Heredia, A. *et al.* Rapamycin causes down-regulation of CCR5 and accumulation of anti-HIV beta-chemokines: an approach to suppress R5 strains of HIV-1. *Proc. Natl. Acad. Sci. USA* **100**, 10411–10416 (2003).
 102. Castedo, M. *et al.* Human immunodeficiency virus 1 envelope glycoprotein complex-induced apoptosis involves mammalian target of rapamycin/FKBP12-rapamycin-associated protein-mediated p53 phosphorylation. *J. Exp. Med.* **194**, 1097–1110 (2001).
 103. Harrington, L.S. *et al.* The TSC1-2 tumor suppressor controls insulin-P13K signaling via regulation of IRS proteins. *J. Cell. Biol.* **166**, 213–223 (2004).
 104. Um, S.H. *et al.* Absence of S6K1 protects against age- and diet-induced obesity while enhancing insulin sensitivity. *Nature* **431**, 200–205 (2004).

XIENCE V™ Everolimus-Eluting Coronary Stent System: A Preclinical Assessment

LAURA E. L. PERKINS, D.V.M., PH.D., D.A.C.V.P., KATRIN H. BOEKE-PURKIS, B.S.,
QING WANG, PH.D., STEVEN K. STRINGER, M.S.,
and LESLIE A. COLEMAN, D.V.M., M.S., D.A.C.L.A.M.

From Abbott Vascular, Santa Clara, California

Background: The XIENCE V™ everolimus-eluting coronary stent system is a second-generation drug-eluting stent designed for safety and efficacy in the interventional treatment of coronary artery disease and in preventing in-stent restenosis. A comprehensive preclinical program was completed to aid in the scientific design and to demonstrate the safety of XIENCE V.

Methods: Studies evaluating clinical dose selection, pharmacokinetics, single and overlapping stent safety, polymer safety, and maximum dose (8× everolimus) safety were conducted in the porcine coronary arterial model at 28, 90, 180 days, and 1 and 2 years. Additionally, a subset of studies was conducted in the rabbit iliac arterial model.

Results: Morbidity and mortality rates for all preclinical studies were exceptionally low, being less than 1%. The arterial response observed in the clinical dose selection study and in all safety studies was typified by benign neointimal hyperplasia with endothelialization by 28 days. Everolimus was released in a controlled manner for 120 days and remained primarily localized within the stented arterial region, which was evidenced histologically as peristrut fibrin. The temporal presence of peristrut fibrin matched the everolimus-elution profile. Thrombosis, malapposition, medial loss, or other adverse effects were not observed in any preclinical studies.

Conclusion: XIENCE V has demonstrated safety via an extremely comprehensive preclinical program published to date for a DES system, with data generated in two species to 2 years. The preclinical data, along with the SPIRIT clinical trial data, demonstrate the excellent safety and potential efficacy profile of XIENCE V. (J Intervent Cardiol 2009;22:S28–S40)

Introduction

The XIENCE™ V everolimus-eluting coronary stent system (Abbott Vascular, Santa Clara, CA) is a second-generation drug-eluting stent (DES) indicated for improving coronary luminal diameter in patients with symptomatic heart disease due to *de novo* native coronary artery lesions and designed to prevent coronary in-stent restenosis. XIENCE V comprises the following four components: the MULTI-LINK VISION® cobalt-chromium, thin-strutted stent; a thin, fluorinated, biocompatible copolymer (PVDF-HFP); the antiproliferative semisynthetic macrolide

everolimus; and the highly flexible ML VISION™ stent delivery system. A comprehensive preclinical safety evaluation has been conducted for the XIENCE V system, including studies in two animal models with up to 2 years' duration of follow-up. The demonstrated safety of XIENCE V in the preclinical setting has been borne out in its outstanding clinical performance in the SPIRIT family of clinical trials.^{1–4} In SPIRIT trials, XIENCE V established itself as unique by being the only US approved DES to twice demonstrate superiority over another [TAXUS® (Boston Scientific, Natick, MA)] in the respective primary end-points of angiographic in-stent and in-segment late loss.^{2–4} In this review, we present the preclinical profile of XIENCE V, including specifically discussions on the pharmacokinetics, single and overlapping stent safety, and the safety of maximum dose and polymer-only constructs.

Address for reprints: Laura E. L. Perkins, D.V.M., M.S., D.A.C.L.A.M., 3200 Lakeside Drive, Santa Clara, CA 95054. Fax: 408-845-4074; e-mail: laura.perkins@av.abbott.com

XIENCE V™ PRECLINICAL ASSESSMENT

Table 1. Summary of Studies Conducted in the Preclinical Evaluation of XIENCE V Everolimus-Eluting Coronary Stent System

Study Type	Preclinical Model	Time Points Evaluated	Balloon: Artery Ratio	Control Arm	Test Arm(s)	Clinical Pathology	QCA	Histology	PK
Clinical dosing	PCA	28 days	1.3:1	VISION	XIENCE V, 200 µg/cm ² EES, 260 µg/cm ² EES	–	X	X	–
Safety	PCA	28, 90, 180 days, 1 and 2 years	1.1:1	VISION	XIENCE V	X	X	X	–
Safety	RIA	28, 90 days	1.2–1.6:1	VISION	XIENCE V	X	X	X	–
Overlapping stent	PCA	28, 90, 180 days	1.1:1	VISION	XIENCE V	X	X	X	–
Overlapping stent	RIA	28, 90 days	1.2–1.6:1	VISION	XIENCE V	X	X	X	–
Max dose	PCA	28, 90, 180 days	1.1:1	VISION	800 µg/cm ² EES	X	X	X	–
Polymer safety	PCA	180 days, 1 and 2 years	1.1:1	VISION	Polymer	X	X	X	–
Bulk polymer	PCA	28, 90, 180 days	1.1:1	VISION	Polymer	X	X	X	–
Pharmacokinetics	PCA	Up to 120 days	1.1:1	–	XIENCE V	X	–	–	X

PCA = porcine coronary arterial model; RIA = rabbit iliac arterial model; EES = everolimus-eluting stent; QCA = quantitative coronary angiography; PK = pharmacokinetics on blood and tissues.

Methods

All experimental studies received protocol approval from the Institutional Animal Care and Use Committee and were conducted in accordance with the American Heart Association (AHA) guidelines for preclinical research and with the Guide for the Care and Use of Laboratory Animals (NIH, 1996). Study procedures were performed in compliance with Good Laboratory Practices (GLP) as defined in the US Code of Federal Regulations, 21 CFR Part 58.^a Animals were maintained on standard porcine or rabbit chow and provided fresh clean water ad libitum. No contaminants were known or assumed to be present in the food or water that could have adversely affected the study outcome.

Studies were conducted in a porcine coronary arterial model (PCA) and a nonatherosclerotic rabbit iliac arterial model (RIA); a summary is provided in Table 1. A high-injury PCA model (balloon:artery ratio, B:A 1.3:1) was used to determine the clinical dose selection. This higher overstretch model was chosen in order to induce a more robust neointimal response for the best assessment of the effectiveness of everolimus at reducing neointimal proliferation.⁵ The pharmacokinetic, single and overlapping stent safety, polymer safety, and maximum dose studies were all conducted as recommended in a low-injury PCA model (B:A 1.1:1).⁶ The 10% overstretch model was used to ensure minimal

damage to the internal elastic lamina for the principal safety assessment of the cellular response and for an *in vivo* characterization of the system's pharmacokinetics. PCA studies were conducted in either juvenile domestic cross-breed farm swine (28, 90 days) or juvenile Yucatan mini-swine (180 days, 1 and 2 years). Additional single and overlapping stent safety studies were conducted in a moderate-injury New Zealand White rabbit iliac model (B:A 1.2–1.6:1; 28, 90 days). Single ML VISION coronary stents were used as controls for the clinical dosing study and single stent safety studies, and overlapping ML VISION stents served as the controls for the overlapping studies.

All animals were treated with aspirin and clopidogrel (Clo) for the duration of the study. Pigs received a loading dose of 325-mg aspirin PO and 150 mg Clo followed by a maintenance of 81-mg aspirin PO sid and 75-mg Clo PO sid. Rabbits were treated with 20-mg aspirin PO sid and 5-mg Clo PO SID.

All procedures (implant and follow-up) were conducted aseptically under general anesthesia. Anesthesia and surgical preparation were conducted per test facility standard operating procedures. Briefly, pigs were anesthetized with Telazol (5–7 mg/kg) intramuscularly, intubated, and maintained under general inhalational anesthesia with isoflurane/oxygen. Rabbits were anesthetized with ketamine (25 mg/kg) intramuscularly, intubated, and maintained under general inhalational anesthesia with isoflurane/oxygen. Whole blood was collected prior to implant and explant for a complete blood count and serum chemistry. All animals were

^a Exception is Dose Selection study, which was conducted non-GLP.

PERKINS, ET AL.

heparinized (100–200 units/kg intravenously) to ensure adequate anticoagulation prior to all procedures. The activated clotting time (ACT) was monitored periodically to ensure appropriate anticoagulation; additional heparin was administered if the ACT <300.

For porcine studies, 3.0 × 12 mm stents were delivered to the coronary arteries via femoral access using standard procedures. The stents were deployed in nontortuous vessel segments that were 2.7–3.2 mm in diameter, using either the 1.1:1 or 1.3:1 B:A as previously described. For rabbit studies, 2.5 × 8 mm stents were delivered to the iliac arteries via carotid access. The carotid artery was isolated and an introducer sheath placed to allow for arterial access. A Swan Ganz catheter was passed over a guidewire through the carotid artery and into the descending abdominal aorta to obtain a baseline angiogram of the iliac arteries. The Swan Ganz catheter was removed, the stent delivery system was advanced over the guidewire, and a stent was delivered into each of the iliac arteries.

Angiographic data were collected pre-stent implant, post-stent deployment, and at the designated study endpoint to allow for assessment of the balloon to artery ratio, thrombolysis in myocardial infarction (TIMI) flow, vessel patency, and the presence of dissections or aneurysms. For safety studies at study termination, a gross pathologic evaluation was performed. All target organs (heart, liver, lung, kidney, spleen) were collected for histopathologic assessment. The stented arteries were collected for a thorough histomorphometric and histopathologic assessment. For pharmacokinetic studies, five XIENCE V lots were tested. Each lot was tested in two animals per time point, with two to three stents implanted per animal. Whole blood samples were collected at multiple time points for analysis of systemic everolimus exposure. At study termination, each stented coronary artery and 5 mm of proximal and distal boundary arterial segments were carefully dissected from the myocardium. Stents were separated from the arterial tissue. Myocardial samples subjacent and distal to stented arteries and representative samples (~1–2 g) from right lung, liver, left kidney, and spleen were collected for everolimus distribution analysis.

Quantitative Coronary Angiography Analysis.

Angiograms were saved to a CD-ROM disk in a standard digital imaging and communications in medicine (DICOM) format. The angiograms were analyzed using a PC-based quantitative coronary angiography (QCA) analysis software program (DICOMview® Angiographic Review Software, Heartlab, Inc., Westerly,

RI). Using the guiding catheter as a reference for calibration, measurements of the baseline vessel diameter, balloon inflated diameter, and the reference vessel diameter and post-stent minimal lumen diameter (MLD) were obtained. The balloon to artery ratio was calculated as the mean balloon-inflated diameter/mean baseline vessel diameter. The percent diameter stenosis was calculated as: $100 \times (1 - [\text{minimal lumen diameter}/\text{reference vessel diameter}])$.

Pharmacokinetic Analysis.

Determination of in vivo release rate. The fractional drug released from the stents over time was determined from differences between the initial drug loading on the stents before implantation and the amount of drug remaining on the explanted stents. Residual everolimus was extracted from stents by the addition of 0.02% BHT/acetonitrile solution. After sonification and filtration, an aliquot of solution was loaded onto a reverse-phase high performance liquid chromatography (HPLC) column for quantification of everolimus in the solution against everolimus calibration standards. The mobile phase of the HPLC column contained acetonitrile, water, and methanol.

Determination of tissue everolimus levels. The everolimus concentration in tissue and blood was determined using liquid chromatography/mass spectrometry (LC/MS). Tissues were homogenized in a dilution solution. After centrifugation, an aliquot of supernatant was injected onto the LC/MS column. A mobile phase gradient containing formic acid and ammonium acetate was used to elute everolimus. The everolimus concentration in tissue was determined by the total amount in dilution solution divided by tissue weight. The limit of quantification of the method is 0.5 ng/mL. For blood, an internal standard (IS)/precipitation solution was added into a whole blood sample. After vortexing and centrifugation, supernatant from the mixture was analyzed by a HPLC column. The limit of quantification of the assay is 0.1 ng/mL.

Histopathologic Analysis. Before processing, the stented porcine coronary arteries and hearts were radiographed using a Faxitron to locate and assess stent placement. Stented arteries were carefully dissected from the myocardium and radiographed again to assess stent deployment and to evaluate for the presence of strut fractures. All implanted rabbit iliac and porcine coronary arteries were routinely processed, embedded in methylmethacrylate, sectioned at 5-μm thickness, and stained with hematoxylin and eosin (HE) or elastic Van Gieson (EVG). A minimum of three cross-sections

XIENCE V™ PRECLINICAL ASSESSMENT

of single stented arterial segments (proximal, mid, and distal), and a minimum of four cross-sections of overlapping stented arterial segments (proximal and distal nonoverlap and two overlapping sections) were collected for histological evaluation. In addition, to evaluate for possible upstream and downstream effects of the stents, segments of the nonstented host artery approximately 5 mm proximal and distal to the stented region were embedded in paraffin, sectioned, and stained with HE and Masson's trichrome (MT).

Two trained pathologists independently reviewed all studies, and a single, trained independent observer generated all quantitative morphometrical and morphological data for each individual study. Both the qualitative and quantitative evaluations were performed in a blinded fashion. Morphometrical evaluations were performed on EVG-stained sections using a digital software program (IP Lab v3.2.4/ Scanalytics, Fairfax, VA), evaluating for lumen area and area within the internal elastic and external elastic lamina (IEL and EEL, respectively). Neointimal area was calculated as the difference between the IEL area and lumen area. Neointimal thickness was measured as the distance from the inner surface of each stent strut to the luminal border. Percent area stenosis was calculated with the formula $[(\text{neointimal area}/\text{IEL area}) \times 100]$. Vessel wall injury scores were determined using the method of Schwartz et al.⁵ Histological sections were evaluated for the presence of luminal thrombus, endothelialization, fibrin deposition, and mineralization based either on the percentage of struts or on an ordinal numerical system (0 = none to minimal, 1 = mild, 2 = moderate, 3 = marked). Inflammation was assessed using the ordinal system of 0 = none to minimal, 1 = mild, 2 = moderate, 3 = marked, 4 = \geq two struts with circumferential to adventitial inflammation.

Following complete fixation, porcine hearts were transversely sectioned at approximately 1-cm intervals to evaluate for gross abnormalities. Histological sections were collected of myocardium immediately subjacent to and distal to the implant site. These myocardial sections were cut at 4–6 μm , mounted and stained with HE, and examined for the presence of infarct, thromboembolus, and inflammation.

Results

Animals were alert and responsive throughout the duration of each study without evidence of abnormal

temperature, weight loss, or other health problems. Blood work remained within normal limits at all time points evaluated. The overall combined mortality rate was <1%. Radiographically, all stents were widely expanded and well apposed to the vessel wall with no incidences of strut fracture.

Clinical Dose Selection. The XIENCE V everolimus-eluting coronary stent system contains 100 $\mu\text{g}/\text{cm}^2$ of everolimus. This formulation was selected based on results obtained from a 28-day clinical dosing study conducted in a high-injury (B:A 1.3:1) porcine coronary arterial model. Three formulations of everolimus-eluting stents (EES) (100 $\mu\text{g}/\text{cm}^2$ with 80% release at 28 days, $n = 11$; 200 $\mu\text{g}/\text{cm}^2$ with 80% release at 28 days, $n = 11$; and 260 $\mu\text{g}/\text{cm}^2$ with 80% released at 60 days, $n = 11$) were compared to an ML VISION metallic stent control ($n = 8$) at 28 days. All three formulations were equally effective at reducing the neointimal response (Fig. 1A). The mean percent area stenosis was markedly reduced ($> 60\%$) for all EES as compared to the ML VISION control. Moreover, all three formulations resulted in similar arterial responses characterized by healthy neointima covering all stent struts. The neointima comprised smooth muscle cells oriented circumferentially in a mild proteoglycan to collagen-based extracellular matrix. Peristrut fibrin, consistent with an everolimus-associated biological effect, and a minimal-to-mild inflammatory response were observed (Fig. 1B). There was no evidence of strut-associated thrombus, medial thinning, or necrosis. All lumens were widely patent and the luminal surfaces were completely endothelialized. Based on these findings, the lowest evaluated effective dose of 100 $\mu\text{g}/\text{cm}^2$ everolimus was chosen for XIENCE V.

Pharmacokinetics.

Everolimus-release profile. The results presented are the average of five XIENCE V lots tested in non-clinical GLP pharmacokinetic studies. The mean cumulative percentage of everolimus released during the first 28 days was approximately 71%, with 29% released during the first 24 hours. Everolimus release reached $\sim 92\%$ by 90 days and was near complete ($95.3 \pm 4.5\%$) by 120 days after stent implantation (Fig. 2A).

Everolimus concentration in tissues. The peak everolimus concentration in stented arterial segments occurred at 3 hours after implantation with a mean of 6.6 ng/mg (Fig. 2B). Everolimus levels were maintained from 2.6 to 0.8 ng/mg from 6 hours to 28 days

PERKINS, ET AL.

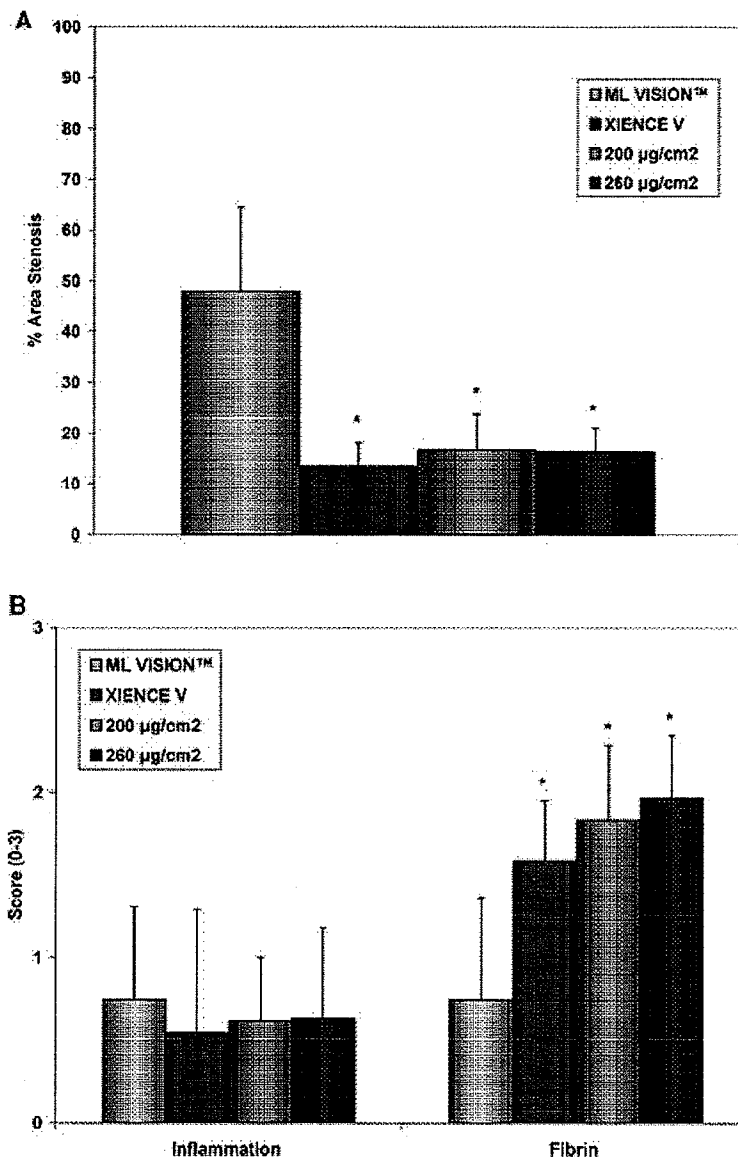


Figure 1. (A) Percent area stenosis obtained in 28-day clinical dosing study conducted in the porcine coronary arterial model. Each evaluated formulation of everolimus-eluting stent system resulted in the significant reduction of percent area stenosis as compared with ML VISION control stent ($P < 0.05$, *). Results presented as mean + standard deviation. The means were compared using one-way analysis of variance. Pair-wise comparisons were performed based on the Student's t-test. (B) Neointimal inflammation and fibrin score obtained in 28-day clinical dosing study conducted in the porcine coronary arterial model. Both inflammation and fibrin were scored using the ordinal numerical system of 0 = none to minimal, 1 = mild, 2 = moderate, 3 = marked. Minimal-to-mild inflammation was obtained for metallic control and each everolimus-eluting formulation evaluated. Mean fibrin scores demonstrate significantly greater peristut fibrin associated with each everolimus-eluting formulation as compared with ML VISION control ($P < 0.05$, *). Results presented as mean + standard deviation. Statistical analysis performed using the nonparametric Wilcoxon (Kruskal-Wallis) rank sum test.

and gradually decreased to 0.2 ng/mg by 120 days postimplantation. Peak levels of everolimus in proximal and distal, nonstented segments were less than 10% of that in stented segments. As expected and relative to arterial flow, everolimus was measurable up to 7 to 14 days in the distal vessel segments but only up to 3 to 7 days in the proximal segments.

Everolimus in the myocardium subjacent to the stented artery was measurable up to 3 to 7 days af-

ter stent implantation, with peak levels between 0.2 and 0.5 ng/mg. In peripheral organs, the drug was either not measurable (below the limit of quantification) at all time points or was measured at only very low levels (0.01–0.02 ng/mg) at 3 hours postimplantation. A trace amount of everolimus was occasionally detected in some organ samples beyond 3 hours. The mean highest everolimus concentration (C_{max}) of five lots in blood was 1.5 ± 0.8 ng/mL at 15 minutes

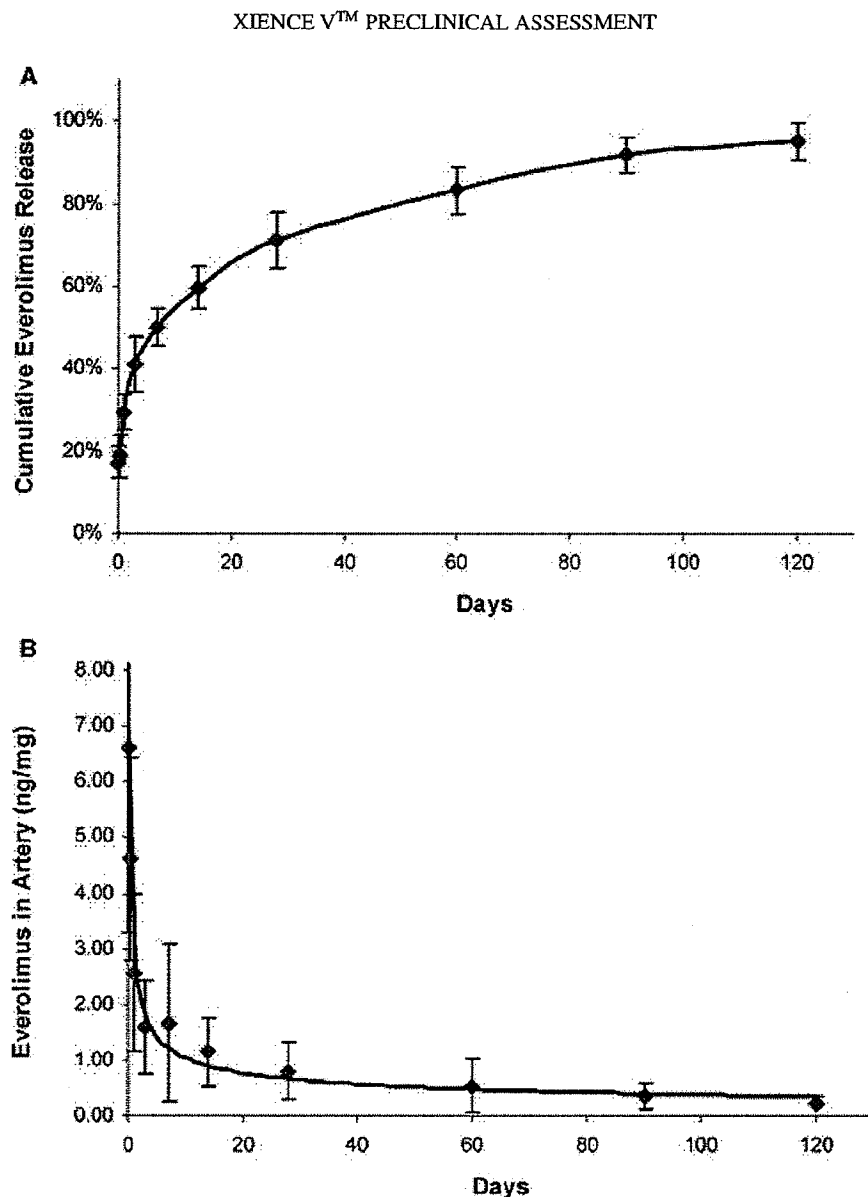


Figure 2. (A) *In vivo* cumulative percent drug-release profile of XIENCE V. Results presented are mean \pm standard deviation, with sample sizes up to 30 per time point. (B) Everolimus concentrations in stented artery following XIENCE V implantation. Results presented are mean \pm standard deviation, with sample sizes up to 30 per time point.

following deployment of three 3.0×12 mm XIENCE V. The blood levels of everolimus quickly declined to below the limit of quantification (<0.1 ng/mL) after 72 hours.

Safety Studies. The safety of XIENCE V was evaluated in both porcine coronary (28, 90, 180 days, 1 and 2 years) and rabbit iliac (28, 90 days) arterial

models. All arteries were angiographically patent and lacked evidence of filling defects, aneurysm formation, dissection, and side-branch occlusion^b at the appointed time of explantation. In the porcine model, ML

^b Side branch pertinent to porcine model only.

PERKINS, ET AL.

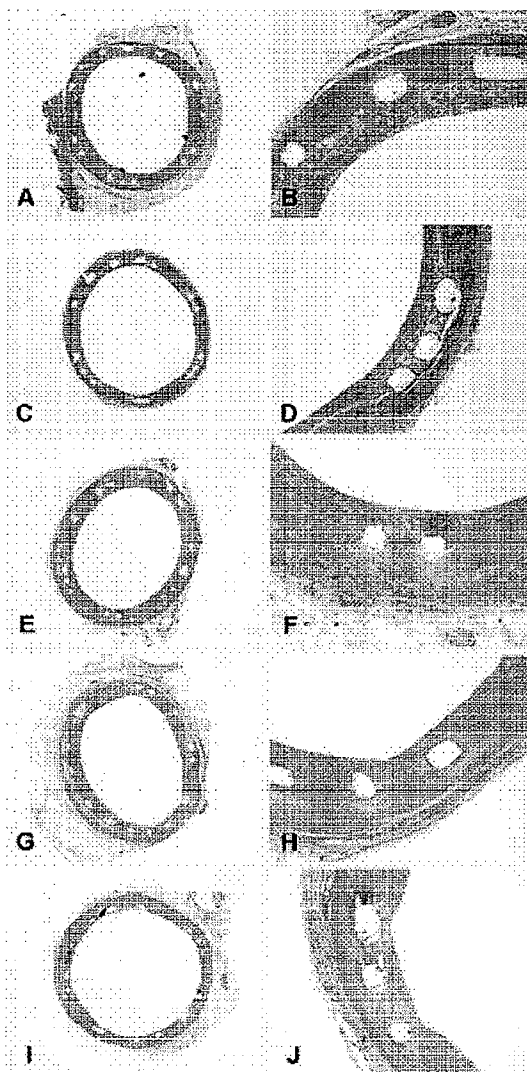


Figure 3. Representative photomicrographs of hematoxylin and eosin-stained sections of porcine coronary arteries 28 days (A, B), 90 days (C, D), 180 days (E, F), 1 year (G, H), and 2 years (I, J) after XIENCE V implantation. Seen are 20 \times (A, C, E, G, I) and 100 \times (B, D, F, H, J) magnifications. Tests performed by and data on file at Abbott Vascular. Photos taken by and data on file at Abbott Vascular.

VISION and XIENCE V had parallel trends in neointimal responses. Specifically, this parallel included a slight decline in neointimal thickness from 28 to 180 days, an appropriate response for this preclinical model that is related to benign arterial remodeling and is consistent with arterial healing. The neointimal thickness for both XIENCE V and ML VISION

remained stable from 180 days to 2 years, indicating that neointimal healing was complete by 180 days. As other DES systems, [CYPHER[®] (Johnson and Johnson, Miami Lakes, FL), TAXUS, and ENDEAVOR[®] (Medtronic Vascular, Inc., Santa Rosa, CA)] have not maintained neointimal suppression when compared to a bare metallic stent in preclinical models beyond 28 days,⁷⁻¹¹ the same quantitative trend was observed in these safety studies between XIENCE V and ML VISION.

Histologically, all arteries had a benign appearance defined by a patent lumen, complete neointimal incorporation of struts, and the absence of main or side-branch thrombus or occlusion^c (Figs. 3 and 4). Endothelialization was complete (>98%) at each time point evaluated for both XIENCE V and ML VISION in both preclinical models. The neointima was composed of parallel aligned smooth muscle cells in early proteoglycan-rich to later collagen-based extracellular matrix. Mild-to-moderate levels of peristrut fibrin were observed at 28 days in XIENCE V-implanted arteries and gradually resolved to absent to rare by 90 to 180 days. The presence of fibrin is attributable to the active phase of localized everolimus elution. Inflammation was of equivalent amount and character for XIENCE V and ML VISION at all time points in both porcine and rabbit models. In porcine studies, at 28 and 90 days, variability was observed among individual animals with respect to inflammation that indicated a tendency for an animal bias. The incidence and character of inflammation observed is similar to that reported for the porcine model in relation to other bare metallic, polymer-coated, and DES coronary stent systems.^{9,11-19} In rabbit studies, neointimal inflammation was very low at both time points and consisted of individual to few macrophages and/or multinucleated giant cells that were largely confined to the neointima and did not affect the underlying media or adventitia. The observed difference in inflammation between rabbit and porcine models at 28 and 90 days suggests a species specific response rather than a device-specific response. At all time points, mineralization was absent to rare for both XIENCE V and ML VISION, and neointimal, medial, and adventitial necrosis and medial thinning were not observed.

No significant lesions were observed in proximal and distal, nonstented host porcine coronary and rabbit iliac

^c Side branch pertinent to porcine model only.

XIENCE V™ PRECLINICAL ASSESSMENT

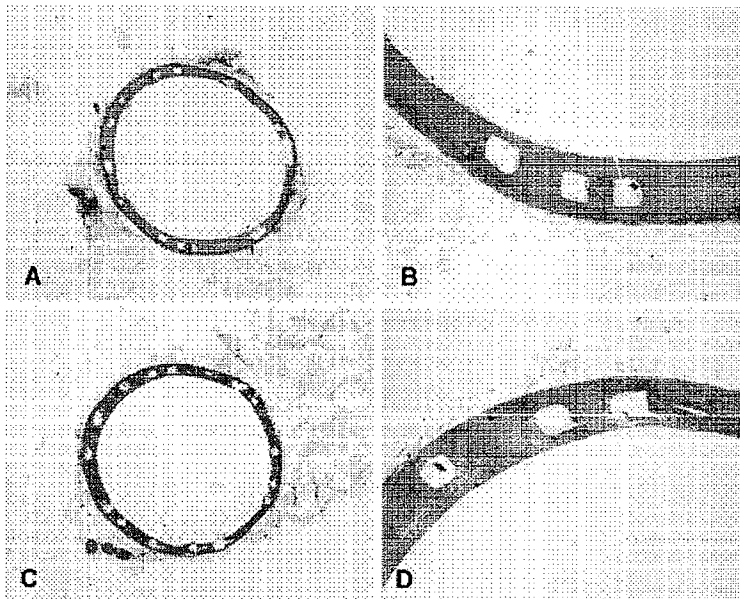


Figure 4. Representative photomicrographs of hematoxylin and eosin-stained sections of rabbit iliac arteries 28 days (A, B) and 90 days (C, D) after XIENCE V implantation. Seen are 20× (A,C) and 100× (B, D) magnifications. Tests performed by and data on file at Abbott Vascular. Photos taken by and data on file at Abbott Vascular.

arteries. In addition, porcine hearts had no significant gross or histological lesions in the myocardium immediately subjacent to or distal to the implanted coronary arteries. These observations indicate that there were no adverse in-segment or distal myocardial effects attributable to the PVDF-HFP polymer or everolimus of XIENCE V.

Overlapping Stent Safety Studies. The safety of overlapping XIENCE V was evaluated in both porcine (28, 90, 180 days) and rabbit (28, 90 days) models by deploying two stents in an overlapping configuration with a minimum of 4-mm stent overlap. Angiographically, there was no evidence of dissection, aneurysm, filling defects, excessive narrowing, thrombosis, or stent migration. Overlapped XIENCE V resulted in a comparable neointimal response as overlapped ML VISION stents, with all stent struts covered by a benign, smooth muscle cell-rich neointima. Each vessel had a patent lumen with complete luminal endothelialization (>98%) by 28 days in both models. There was no evidence of luminal, strut-associated, or side-branch thrombus at any time point.^d As demonstrated with the single stent safety studies, an active biological effect secondary to the elution of everolimus was evidenced in both models at 28 days by mild-to-

moderate peristrut fibrin, which rapidly resolved by 180 days. Minimal, localized mineralization was absent to rare for both models. Medial thinning, medial necrosis, or other localized adverse effects were not observed. As expected for the respective models, no-to-minimal inflammation was observed in association with both the XIENCE V and ML VISION overlapping stent systems in the rabbit model, whereas inflammation was variably associated with both overlapping stent systems in the porcine model principally at 28 and 90 days, being much resolved by 180 days. Inflammation in the porcine model was of a similar nature and animal predilection as observed in the single stent safety studies described previously. The porcine model demonstrated a marginal reduction of neointimal thickness and percent area stenosis from 28 to 180 days for both overlapping devices relative to benign arterial remodeling that normally occurs.

Maximum Dose Safety Studies. The safety of a maximum dose EES was evaluated in a low-injury porcine coronary artery model (28, 90, 180 days) to determine the safety margin of XIENCE V. The maximum dose EES contained 800 $\mu\text{g}/\text{cm}^2$ everolimus, eight times the dose density of everolimus in XIENCE V. The release kinetics of the maximum dose EES was determined to be similar to XIENCE V, with 80% of the total drug load released by 28 days. As expected, higher initial arterial tissue concentrations of everolimus were

^d Side branch pertinent to porcine model only.

PERKINS, ET AL.

measured following implantation with the maximum dose EES. Despite higher arterial tissue concentrations, patent lumens with TIMI 3 flow were observed angiographically at all time points evaluated. The vascular response was benign, with no evidence of drug-associated vascular toxicity, thus demonstrating a wide safety window. All stent struts were covered with a smooth muscle cell-rich neointima, similar to that observed in the porcine safety studies. A localized effect of everolimus was evidenced in the vessel wall as mild-to-moderate peristrut fibrin at 28 days. All vessels demonstrated complete luminal endothelialization (>99%). There was no evidence of luminal thrombus or strut-associated thrombus at any time point. Medial thinning and medial necrosis also were not observed.

Polymer Studies. The biocompatibility of a 1X polymer-only construct (equivalent to XIENCE V) was studied at 180 days and 1 and 2 years, and that of a 3X polymer-only construct was studied at 28, 90, and 180 days. Angiographic and histological results in porcine coronary arteries for polymer-coated stents were equivalent to the ML VISION stent at all time points. Vessels retained a patent lumen with all stent struts incorporated in an endothelialized, smooth muscle cell-rich neointima, with no evidence of aneurysm, main or side-branch thrombosis, medial thinning, or necrosis at any time point. Inflammation associated with polymer-only stents paralleled that of ML VISION-implanted arteries, being negligible to mild from 28 days to 2 years. Furthermore, evidence of delamination of the XIENCE V fluorinated copolymer (PVDF-HFP) was not apparent in implanted arteries at any time.

Discussion

The XIENCE V everolimus-eluting coronary stent system is a second-generation DES designed to address both safety and efficacy in the interventional treatment of coronary artery disease and in preventing in-stent restenosis. In this review, we have presented a summary of the comprehensive XIENCE V preclinical program, which has included studies of duration up to 2 years and in two accepted preclinical models in order to account for any species specific responses.^{6,9} In addition to illustrating XIENCE V safety in both single and overlapping applications, the broad safety margin of everolimus has been established in studies with a maximum dose system (8× everolimus) to 6 months, and

the biocompatibility of PVDF-HFP polymer has been demonstrated in studies with bulk (3X) and single (1X) load polymer-only constructs to 6 months and 2 years, respectively.

The safety of XIENCE V has been exemplified by the similarity of the vascular response of both rabbit iliac and porcine coronary arteries to XIENCE V and ML VISION. The vascular response to both devices included complete endothelialization and complete neointimal incorporation of struts by 28 days with no evidence of thrombosis, positive remodeling, medial necrosis, or strut malapposition. The chief distinguishing feature between XIENCE V and ML VISION was the presence of mild peristrut fibrin associated with XIENCE V, which was observed mainly at 28 days, had largely resolved by 90 days, and therefore was in accordance with the everolimus-elution and tissue-retention profiles determined in pharmacokinetic studies. Stable vascular responses were demonstrated from 6 months to 2 years, indicating that arterial healing had occurred by and was maintained beyond 6 months. In addition to the benign responses within the stented artery, in-segment rabbit and porcine host arteries were normal with no evidence of adverse edge effects, and porcine myocardium distal to the implant sites had no adverse lesions.

XIENCE V consists of four components, each of which has been optimized to allow arterial healing while reducing in-stent restenosis. First, XIENCE V is built on the foundation of the ML VISION thin-strut cobalt-chromium stent, the best-selling bare metallic stent worldwide.²⁰ With this is the second component of XIENCE V, the ML VISION stent delivery system, which is designed for optimal deliverability. The cobalt-chromium composition of the ML VISION stent allows for thinner struts without compromise to its radio-opacity or radial strength. The ML VISION design allows for optimal vessel wall scaffolding due to its flexibility and conformability, an important feature for ensuring good stent-to-vessel wall apposition upon deployment to minimize the risk of acute thrombus formation.²¹ In addition to inducing less thrombus, the thin struts of the ML VISION stent also are designed to induce less injury to the vessel wall, with both thrombus and injury being important factors influencing neointimal proliferation and restenosis.^{5,22} The benefit of thin-strut stents has been demonstrated clinically in the ISAR-STEREO and ISAR-STEREO 2 trials in which thin-strut stents were associated with a significant reduction in angiographic and clinical

XIENCE V™ PRECLINICAL ASSESSMENT

restenosis as compared to thick-strut stents.^{23,24} Finally, as less neointima is likely required to cover a thin-strut stent, moreover, thin struts also will likely endothelialize more rapidly than thick struts, as has been indicated in studies in *ex vivo* and rabbit iliac arterial models.^{25,26}

The third component of XIENCE V is everolimus, an immunosuppressive macrolide acting as an mTOR (mammalian target of rapamycin) inhibitor.²⁷ As a result of its action, select hematopoietic and non-hematopoietic cells (e.g., vascular smooth muscle cells) are arrested in the G1 phase of the cell cycle. Oral administration of everolimus (Certican®) in renal and heart transplant patients has been extensively studied.²⁸⁻³⁰ At therapeutic doses, the minimal blood concentration (C_{min}) is 3 ng/mL (trough concentrations 4.3 ng/mL to 7.2 ng/mL),^{31,32} well above the measurable blood concentrations obtained in these preclinical studies. Importantly, the preclinical pharmacokinetics are consistent with the measured profiles obtained clinically in the SPIRIT II and SPIRIT III pharmacokinetic substudies.³³ In XIENCE V, the lowest effective dose of everolimus was incorporated in the system to allow for the balance of rapid vessel healing with the reduction of vascular smooth muscle cell proliferation. In the porcine coronary arterial model, XIENCE V reproducibly displayed a well-controlled everolimus-release profile distinct from the fast-release kinetics of ENDEAVOR and the slow-release profile of TAXUS.³⁴⁻³⁶ As the release kinetics of XIENCE V corresponds with the key cellular phases of vascular healing,^{37,38} the system rendered an efficient delivery of everolimus to the coronary arterial wall, with sufficient concentration maintained for 28 days following implantation for effective inhibition of vascular smooth muscle cell proliferation. Histologically, this was evidenced by the maximal presence of peristrut fibrin at 28 days. Furthermore, the XIENCE V releases everolimus within 120 days to allow for complete vascular healing. Again, the correlation between pharmacokinetics and the vascular response was confirmed both by the largely complete resolution of fibrin by 90 days and by the vascular quiescence observed from 6 months to 2 years. This contrasts to what has been observed with TAXUS, as its slower and more indefinite release of cytotoxic paclitaxel may account for the medial loss and excess fibrin deposition that has been observed in preclinical models^{11,39} and has been clinically reflected by excess fibrin with or without strut malapposition.^{40,41}

The fourth and final component of the XIENCE V is the PVDF-HFP polymer, a benign fluoropolymer that has been used in other vascular and nonvascular applications.³³ The principal end-points of the preclinical safety studies evaluating the PVDF-HFP polymer were to establish its long-term safety and integrity, as for all durable polymer-based DES systems, these two factors have been the source of recent apprehensions in the clinical setting.⁴² Long-term safety was established in the preclinical studies using both single (1X) and bulk (3X) polymer constructs of XIENCE V, as there was similarity in the vascular responses of porcine coronary arteries to the ML VISION control and the polymer-only constructs from 28 days to 2 years. Of particular note were the comparably low levels of inflammation observed at all time points. This contrasts to observations made in association with CYPHER, to which increased inflammation with time has been noted in both the porcine coronary and rabbit iliac arterial models.^{7,9,16,39,43,44} Further, this inflammation observed in preclinical models may be mirrored by the inflammation observed clinically in association with cases of late stent thrombosis for this DES.^{13,40,41,45} As the elution profiles for CYPHER and XIENCE V are comparable, with complete sirolimus elution 90 days, this late inflammation for CYPHER has been primarily attributed to the polymer.^{13,44-46} In addition to polymer safety, polymer integrity of XIENCE V and polymer-only constructs also were demonstrated in these studies. The PVDF-HFP polymer remained intact with no evidence of delamination or migration into the adjacent arterial or distal myocardial tissues in histological sections. Conversely, polymer delamination has been observed in preclinical studies involving other DES systems.⁴⁷ Though the clinical implications of poor polymer integrity or polymer delamination are as yet unknown, our rapidly advancing understanding of DES system is certain to offer insight in the near future.

The combination of thin struts (Fig. 5), reduced everolimus load, and the biocompatible durable PVDF-HFP polymer of the XIENCE V EECSS contributes to overall rapid vessel healing characterized by a consistent and benign neointimal response over time. The rapid healing response was further demonstrated in rabbit arterial endothelialization studies wherein XIENCE V demonstrated more rapid endothelial cell recovery as compared to ENDEAVOR, CYPHER, and TAXUS LIBERTE drug-eluting stents (Fig. 6).⁴⁸ In this model, XIENCE V-implanted arteries demonstrated

PERKINS, ET AL.

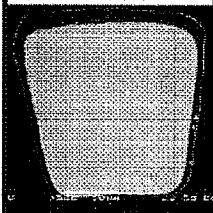
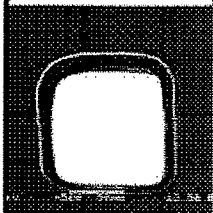
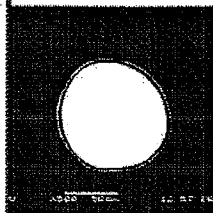
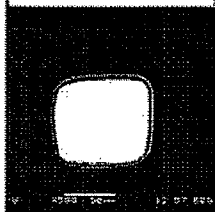
CYPHER®	TAXUS® Liberté	ENDEAVOR™	XIENCE V™
			
Strut Thickness: 140µm	Strut Thickness: 97µm	Strut Thickness: 91µm	Strut Thickness: 81µm
Polymer Thickness: 12.6µm	Polymer Thickness: 17.8µm	Polymer Thickness: 4.8µm	Polymer Thickness: 7.8µm

Figure 5. Schematic of scanning electron micrograph cross-sections of 3.0-mm diameter CYPHER, TAXUS Liberté, ENDEAVOR, and XIENCE V stent systems, demonstrating the overall thin strut and polymer coating of XIENCE V (500× magnification of single strut in cross-section).

significantly greater endothelial coverage over the stent struts at 14 days as compared to the other DES. This coverage was confirmed by greater expression of platelet endothelial cell adhesion molecule (PECAM-1), indicating the presence of a more mature endothe-

lium, as well as decreased vascular endothelial cell growth factor (VEGF) consistent with an intact endothelialized surface observed with the XIENCE V. Thus, the XIENCE V, a second-generation DES, is associated with the essential features of optimal vessel

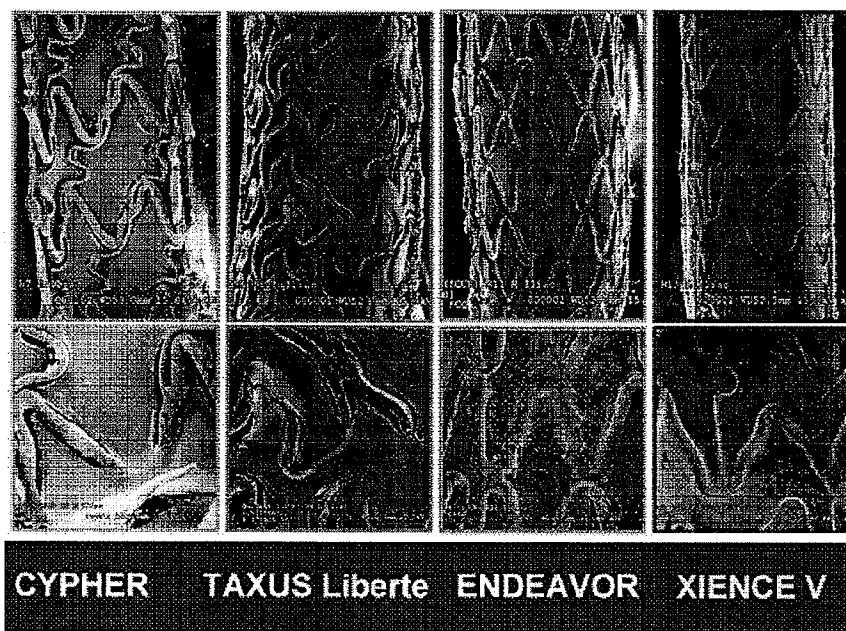


Figure 6. Representative scanning electron micrographs of the luminal surface of rabbit iliac arteries implanted with CYPHER, TAXUS Liberté, ENDEAVOR, and XIENCE V DES for 14 days demonstrating greater overall endothelial cell coverage with XIENCE V (low-magnification images at 15×; inserts at 200× magnification).

XIENCE V™ PRECLINICAL ASSESSMENT

healing in preclinical models: rapid reendothelialization and the formation of a benign neointimal response with all struts incorporated.

Limitations. Though the stages of vascular healing following stent application are similar, the vascular effects of DES systems in preclinical arterial models are not necessarily predictive of those that occur in atherosclerotic, aged human coronary arteries.^{6,37} The purpose of these studies was to evaluate in standard preclinical models the safety, biocompatibility, and pharmacokinetics of XIENCE V, with an understanding of this limitation toward clinical relevance. Herein, XIENCE V, implanted in either single or overlapping fashion, fulfilled these preclinical objectives, by demonstrating vascular healing and safety comparable to ML VISION to 2 years in the porcine coronary arterial model and to 90 days in the rabbit iliac arterial model, with no adverse effects, such as late stent thrombosis, excess inflammation, or polymer delamination, being noted.

Conclusions

The XIENCE V everolimus-eluting coronary stent system is unique among DES approved in the United States, both for its demonstration of superior angiographic outcomes in the SPIRIT family of clinical trials¹⁻³ as well as for its demonstrated preclinical safety profile, which has been established by the most thorough and long-term preclinical evaluation published to date for a DES system.^{7,9,11} Complete endothelialization, sequestration of struts within a benign, fibromuscular neointima, a widely patent lumen, and low inflammation typified the vascular responses to single and overlapping XIENCE V in two animal models. Furthermore, arterial responses were in direct parallel with the system's pharmacokinetics, with complete vascular healing by 6 months in accordance with complete everolimus elution.

References

1. Beijk MA, Piek JJ. XIENCE V everolimus-eluting coronary stent system: A novel second generation drug-eluting stent. *Expert Rev Med Devices* 2007;4:11-21.
2. Serruys PW. SPIRIT II study: A clinical evaluation of the XIENCE V everolimus eluting coronary stent system in the treatment of patients with de novo native coronary artery lesions. Late-breaking clinical trials 3. Presented at the American College of Cardiology Scientific Sessions/12 Summit-SCAI Annual Meeting, 2008.
3. Stone GW, Midei M, Newman W, et al. Comparison of an everolimus-eluting stent and a paclitaxel-eluting stent in patients with coronary artery disease: A randomized trial. *JAMA* 2008;299:1903-1913.
4. Stone GW, Murphy SA, Gibson CM. SPIRIT III. *ACC CardioSource Rev J* 2007;16:43.
5. Schwartz RS, Huber KC, Murphy JG, et al. Restenosis and the proportional neointimal response to coronary artery injury: Results in a porcine model. *J Am Coll Cardiol* 1992;19:267-274.
6. Schwartz RS, Edelman ER, Carter A, et al. Drug-eluting stents in preclinical studies: Recommended evaluation from a consensus group. *Circulation* 2002;106:1867-1873.
7. Carter AJ, Aggarwal M, Kopia GA, et al. Long-term effects of polymer-based, slow-release, sirolimus-eluting stents in a porcine coronary model. *Cardiovasc Res* 2004;63:617-624.
8. Cilingiroglu M, Elliott J, Patel D, et al. Long-term effects of novel biolimus eluting DEVAX AXCESS plus nitinol self-expanding stent in a porcine coronary model. *Catheter Cardiovasc Interv* 2006;68:271-279.
9. Nakazawa G, Finn AV, John MC, et al. The significance of pre-clinical evaluation of sirolimus-, paclitaxel-, and zotarolimus-eluting stents. *Am J Cardiol* 2007;100:36M-44M.
10. Salu KJ, Bosmans JM, Bult H, et al. Drug-eluting stents: A new treatment in the prevention of restenosis. Part I: Experimental studies. *Acta Cardiol* 2004;59:51-61.
11. Wilson GJ, Polovick JE, Huibregtse BA, et al. Overlapping paclitaxel-eluting stents: Long-term effects in a porcine coronary artery model. *Cardiovasc Res* 2007;76:361-372.
12. De Scheerder IK, Wilczek KL, Verbeken EV, et al. Biocompatibility of polymer-coated oversized metallic stents implanted in normal porcine coronary arteries. *Atherosclerosis* 1995;114:105-114.
13. Finn AV, Nakazawa G, Joner M, et al. Vascular responses to drug eluting stents: Importance of delayed healing. *Arterioscler Thromb Vasc Biol* 2007;27:1500-1510.
14. Karas SP, Gravanis MB, Santoian EC, et al. Coronary intimal proliferation after balloon injury and stenting in swine: An animal model of restenosis. *J Am Coll Cardiol* 1992;20:467-474.
15. Rodgers GP, Minor ST, Robinson K, et al. The coronary artery response to implantation of a balloon-expandable flexible stent in the aspirin- and non-aspirin-treated swine model. *Am Heart J* 1991;122:640-647.
16. Schwartz RS, Wilson GJ. CYPHER versus TAXUS stents: Comparing the inflammatory response in porcine coronary arteries. TCT (Abstract), *Am J Cardiol* 2006;98:36M.
17. Touchard AG, Schwartz RS. Preclinical restenosis models: Challenges and successes. *Toxicol Pathol* 2006;34:11-18.
18. Van Der Giessen WJ, Lincoff AM, Schwartz RS, et al. Marked inflammatory sequelae to implantation of biodegradable and nonbiodegradable polymers in porcine coronary arteries. *Circulation* 1996;94:1690-1697.
19. Yorozya M, Suzuki H, Iso Y, et al. Comparison of the morphological changes of restenosis after the implantation of various types of stents in a swine model. *Coron Artery Dis* 2002;13:305-312.
20. US Market Overview Report. PGM, Inc. December 2007.
21. Garasic JM, Edelman ER, Squire JC, et al. Stent and artery geometry determine intimal thickening independent of arterial injury. *Circulation* 2000;101:812-818.
22. Schwartz RS, Holmes DR Jr, Topol EJ. The restenosis paradigm revisited: An alternative proposal for cellular mechanisms. *J Am Coll Cardiol* 1992;20:1284-1293.
23. Kastrati A, Mehilli J, Dirschinger J, et al. Intracoronary stenting and angiographic results: Strut thickness effect on restenosis

PERKINS, ET AL.

- outcome (ISAR-STEROE) trial. *Circulation* 2001;103:2816–2821.
24. Pache J, Kastrati A, Mehilli J, et al. Intracoronary stenting and angiographic results: Strut thickness effect on restenosis outcome (ISAR-STEROE-2) trial. *J Am Coll Cardiol* 2003;41:1283–1288.
 25. Simon C, Palmaz JC, Sprague EA. Influence of topography on endothelialization of stents: Clues for new designs. *J Long Term Eff Med Implants* 2000;10:143–151.
 26. Nakazawa G, Kolodgie F, Virmani R. 2008; Data on file.
 27. Schuler W, Sedrani R, Cottens S, et al. SDZ RAD, a new rapamycin derivative: Pharmacological properties in vitro and in vivo. *Transplantation* 1997;64:36–42.
 28. Eisen HJ, Tuzcu EM, Dorent R, et al. Everolimus for the prevention of allograft rejection and vasculopathy in cardiac-transplant recipients. *N Engl J Med* 2003;349:847–858.
 29. Kaplan B, Tedesco-Silva H, Mendez R. North/South American, double-blind, parallel group study of the safety and efficacy of Certican. *Am J Transplant* 2001;1:475.
 30. Vitko S, Margreiter R, Weimar W. International, double-blind, parallel group study of the safety and efficacy of CerticanTM (RAD) versus mycophenolate mofetil in combination with Neoral[®] and steroids. *Am J Transplant* 2001;1:474.
 31. Kovarik JM, Kaplan B, Silva HT, et al. Pharmacokinetics of an everolimus-cyclosporine immunosuppressive regimen over the first 6 months after kidney transplantation. *Am J Transplant* 2003;3:606–613.
 32. Kovarik JM, Kaplan B, Tedesco Silva H, et al. Exposure-response relationships for everolimus in de novo kidney transplantation: Defining a therapeutic range. *Transplantation* 2002;73:920–925.
 33. Johnson G. XIENCETM V everolimus eluting coronary stent system (EECSS): PMA # P070015, 2007. <http://www.fda.gov/ohrms/dockets/ac/07/slides/20007-4333s-00-index.html>.
 34. Leon MB. ENDEAVOR IV: A randomized comparison of a zotarolimus eluting stent and a paclitaxel eluting stent in patients with coronary artery disease. TCT 2007.
 35. Mehta RH, Leon MB, Sketch MH Jr. The relation between clinical features, angiographic findings, and the target lesion revascularization rate in patients receiving the Endeavor zotarolimus-eluting stent for treatment of native coronary artery disease: An analysis of ENDEAVOR I, ENDEAVOR II, ENDEAVOR II Continued Access Registry, and ENDEAVOR III. *Am J Cardiol* 2007;100:62M–70M.
 36. Kamath KR, Barry JJ, Miller KM. The Taxus drug-eluting stent: A new paradigm in controlled drug delivery. *Adv Drug Deliv Rev* 2006;58:412–436.
 37. Virmani R, Kolodgie FD, Farb A, et al. Drug eluting stents: Are human and animal studies comparable? *Heart* 2003;89:133–138.
 38. Forrester JS, Fishbein M, Helfant R, et al. A paradigm for restenosis based on cell biology: Clues for the development of new preventive therapies. *J Am Coll Cardiol* 1991;17:758–769.
 39. Finn AV, Kolodgie FD, Hamek J, et al. Differential response of delayed healing and persistent inflammation at sites of overlapping sirolimus- or paclitaxel-eluting stents. *Circulation* 2005;112:270–278.
 40. Joner M, Finn AV, Farb A, et al. Pathology of drug-eluting stents in humans: Delayed healing and late thrombotic risk. *J Am Coll Cardiol* 2006;48:193–202.
 41. Virmani R. Histopathology of in-human atherosclerotic healing response in BMS and first generation S. DE Proceedings of the International Local Drug Delivery Meeting and Cardiovascular Course on Revascularization and Molecular Strategies, 2008.
 42. Luscher TF, Steffel J, Eberli FR, et al. Drug-eluting stent and coronary thrombosis: Biological mechanisms and clinical implications. *Circulation* 2007;115:1051–1058.
 43. Nakazawa G, Finn AV, Virmani R. Vascular pathology of drug-eluting stents. *Herz* 2007;32:274–280.
 44. Nakazawa G, Finn AV, Ladich E, et al. Drug eluting stent safety: Findings in preclinical studies. *Expert Rev Cardiovasc Ther* 2008;6:1379–1391.
 45. Virmani R, Guagliumi G, Farb A, et al. Localized hypersensitivity and late coronary thrombosis secondary to a sirolimus-eluting stent: Should we be cautious? *Circulation* 2004;109:701–705.
 46. Virmani R, Farb A, Guagliumi G, et al. Drug-eluting stents: Caution and concerns for long-term outcome. *Coron Artery Dis* 2004;15:313–318.
 47. Perkins LEL, Sheehy AS, Coleman LA, et al. XIENCETM V, TAXUS[®], and ENDEAVOR[®] drug eluting coronary stent systems: Comparison in the rabbit iliac arterial model TCT (Abstract). *Am J Cardiol* 2008;102:126i.
 48. Joner M, Nakazawa G, Finn AV, et al. Endothelial cell recovery between comparator polymer-based drug-eluting stents. *J Am Coll Cardiol* 2008;52:333–342.

MAIN Ser CISTI/ICIST NRC/CNRC
QP89 MAIN Ser
T76 0041-1337
v. 64 Received on: 08-07-97
no. 1 Transplantation.
Jul 15,
1997

antation®

Transplantation.
Faxon Stacks M-55

July 15, 1997

OVERVIEW

Balancing the immune system for tolerance:
a case for regulatory CD4 cells

H.H. Field, Q. Gao, N. Chen, and T.M. Rouse

Transplantation
Faxon Stacks M-55

Transplantation
Faxon Stacks M-55

CORD078382

Transplantation[®]

OFFICIAL JOURNAL OF THE TRANSPLANTATION SOCIETY

Editors

J. R. BATCHELOR
London, England
ANTHONY P. MONACO
Boston, Massachusetts

EUROPEAN EDITORIAL OFFICE:
Nuffield Department of Surgery
University of Oxford
John Radcliffe Hospital
Headington, Oxford OX3 9DU, U.K.

PETER J. MORRIS
Oxford, England
DAVID H. SACHS
Boston, Massachusetts

NORTH AMERICAN EDITORIAL OFFICE:
New England Deaconess Hospital
1 Deaconess Road
Boston, Massachusetts 02215, U.S.A.

MANIKKAM SUTHANTHIRAN
New York, New York
KATHRYN J. WOOD
Oxford, England

Emeritus Editors

ERNST J. EICHWALD
HERBERT CONWAY
NATHAN KALISS
LESLIE BRENT
JOSEPH E. MURRAY
JAMES G. HOWARD
ARNOLD R. SANDERSON
DAVID STEINMULLER
MARY L. WOOD

Editorial Board

M. ABECCASSI
D. ADAMS
J. W. ALEXANDER
P. AMLOT
A. ANDERSSON
A. D'APICE
H. AUCHINCLOSS
J. M. AUSTYN
A. BARRAN
J. C. BALDWIN
W. M. BALDWIN
C. BANGHAM
C. F. BARKER
W. A. BAUMGARTNER
E. BELL
P. BELL
W. E. BESCHORNEN
M. E. BILLINGHAM
A. BISHOP
D. K. BISHOP
B. R. BLAZAR
J. A. BLUESTONE
K. BLUME
E. BOLTON
J. A. BRADLEY
J. D. BRIGGS
J. S. BROMBERG
C. BUNCH
W. J. BURLINGHAM
L. J. BURNS
A. BUSHNELL
R. W. BUSUTTIL
R. CALNE
J. CHAPMAN
B. CHARPENTIER
L. CHATELON
S. I. CHO
F. CLAAS
S. CORBOLD
J. COHEN
R. B. COLVIN
C. CONLON
A. COORE
D. K. C. COOPER
A. B. COSIMI
D. V. CRAMER
D. CRAWFORD
J. J. CUKTIS

A. P. DALMASSO
H. J. DIEG
F. L. DELMONTEO
J. DEVLIN
M. DONAGHY
J. S. DUMMER
D. L. DORN
R. J. DUQUESNOY
P. DYER
R. B. EPSTEIN
C. O. ESQUIVEL
R. B. ETTEGER
J. FARR
O. FARGES
J. L. M. FERRARA
E. H. FIELD
R. N. FINE
O. J. FINN
M. B. FIRST
J. FIRTH
S. M. FLECHNER
M. W. FLYE
J. D. FRELINGER
E. A. FRIEDMAN
P. FRIEND
S. FUGGLE
B. J. FULLER
T. C. FULLER
A. O. GABER
M. R. GAROVVOY
R. L. GELLER
R. G. GILL
N. E. GOKKEN
J. M. GOLDMAN
M. GOLDMAN
G. J. GORES
E. GOULMY
J. J. GOZZO
D. GRANT
D. GRAY
R. E. GRESS
C. GBOU
R. D. GUTTMANN
G. A. HADLEY
P. F. HALLORAN
S. M. HAMMER
W. W. HANCOCK
J. A. HANSEN

D. W. HANTO
M. A. HARDY
W. HARMON
D. HART
D. HASKARD
P. HAYRY
J. H. HELDKERMAN
A. D. HESS
R. HIGGINS
D. HOLT
J. D. HOSENFUD
D. A. HULLETT
S. HUNT
S. T. ILDSTAD
P. JABLONSKI
R. F. L. JAMES
N. JAMIESON
M. JEANNET
B. JOHNSON
M. L. JORDAN
M. A. JOTILA
B. D. KAHAN
M. P. KAYE
R. H. KIERMAN
R. KHAOLI
U. KHETTRY
J. A. KIRBY
B. L. KIRKMAN
G. B. KLINTMALM
S. J. KNECHTLE
R. A. P. KOENE
G. KOOTSTRA
R. KORNIGOLD
S. M. KRAMS
H. KREIS
R. A. F. KROM
I. L. KRON
J. W. KUPIEC-WEGLINSKI
J. B. KURTZ
R. LECHLER
G. S. LEFKOWITZ
G. LOMBARDI
R. P. LOWRY
S. V. LYNCH
A. MADRIGAL
T. MANDEL
R. MARGREITER
M. MARTIN

D. W. MASON
A. J. MATAS
C. G. A. MCGREGOR
I. MCKENZIE
A. MCLEAN
P. MCMASTER
R. W. MELVOLD
S. METCALFE
D. MIDDLETON
C. M. MILLER
J. MILLER
C. MILLER-GRAZIANO
T. MOHANAKUMAR
E. MOLLER
R. E. MORRIS
A. NAJ
G. NEILD
J. NEUBERGER
D. J. NORMAN
A. C. NOVICK
J. B. O'CONNELL
G. OPELZ
C. G. OROSZ
L. C. PAUL
T. PEANSON
D. PEGG
I. PENN
J. PEPPER
J. D. PERKINS
M. PESCOVITZ
M. R. PITTELKOW
J. L. PLATT
J. PROP
N. L. REINSMOEN
C. RICORDI
O. RINGDEN
J. ROAKE
R. J. ROHRER
K. ROLLES
D. ROOPENIAN
M. L. ROSE
J. C. ROSENBERG
H. H. RUBIN
M. E. RUSSELL
D. R. SALOMON
O. SALVATERRA
M. SANDRIN
F. P. SANFILIPPO

C. SAVAGE
M. H. SAYEGH
J. C. SCORNIK
D. A. SEDMAK
R. SELLS
D. SHAFFER
A. SHARER
B. W. SHAW, JR.
A. G. R. SHELL
H. SHENKIN
D. SHOESKEES
R. L. SIMMONS
E. SIMPSON
D. R. SNYDMAN
H. W. SOLLINGER
J. H. SOUTHWARD
A. SPENCER
T. E. STANZL
R. STORF
S. M. STRASBERG
R. J. STRATTA
J. W. STREILEIN
D. E. R. SUTHERLAND
M. SYKES
C. TAYLOR
R. TAYLOR
A. TEJANI
P. I. TERASAKI
J. M. THOMAS
A. W. THOMSON
N. L. TILNEY
A. TING
J. TREDGER
G. TUFVESON
L. A. TURKA
J. D. TYLER
A. G. TZAKIS
D. A. VALLERA
G. B. VOGELIANG
M. WAER
J. WALLWORK
G. L. WARKOCK
A. WARRENS
D. WHITE
R. WILLIAMS
R. F. M. WOOD
R. P. WOOD
A. ZEEVI

CORD078383

0041-1837/97/8401-36\$03.00/0
TRANSPLANTATION
Copyright © 1997 by Williams & Wilkins

Vol. 64, 36-42, No. 1, July 16, 1997
Printed in U.S.A.

SDZ RAD, A NEW RAPAMYCIN DERIVATIVE

PHARMACOLOGICAL PROPERTIES IN VITRO AND IN VIVO

WALTER SCHULER,^{1,2} RICHARD SEDRANI,¹ SYLVAIN COTTENS,¹ BARBARA HÄBERLIN,³
MANFRED SCHULZ,¹ HENK-JAN SCHUURMAN,¹ GERHARD ZENKE,¹ HANS-GÜNTER ZERWES,¹
AND MAX H. SCHREIER¹

Preclinical Research, and Technical Research and Development, Novartis Pharma AG, CH-4002 Basel, Switzerland

Background. This report describes the preclinical pharmacological profile of the new rapamycin analog, SDZ RAD, i.e., 40-O-(2-hydroxyethyl)-rapamycin.

Methods. The pharmacological effects of SDZ RAD were assessed in a variety of in vitro and in vivo models, which included an autoimmune disease model as well as kidney and heart allotransplantation models using different rat strain combinations.

Results. SDZ RAD has a mode of action that is different from that of cyclosporine or FK506. In contrast to the latter, SDZ RAD inhibits growth factor-driven cell proliferation in general, as demonstrated for the in vitro cell proliferation of a lymphoid cell line and of vascular smooth muscle cells. SDZ RAD is immunosuppressive in vitro as demonstrated by the inhibition of mouse and human mixed lymphocyte reactions and the inhibition of antigen-driven proliferation of human T-cell clones. The concentrations needed to achieve 50% inhibition in all of these assays fall into the subnanomolar range. SDZ RAD is effective in the in vivo models when given by the oral route in doses ranging between 1 mg/kg/day and 5 mg/kg/day. When compared with rapamycin, the in vitro activity of SDZ RAD is generally about two to three times lower; however, when administered orally, SDZ RAD is at least as active in vivo as rapamycin.

Conclusions. In conclusion, SDZ RAD is a new, orally active rapamycin-derivative that is immunosuppressive and that efficiently prevents graft rejection in rat models of allotransplantation. SDZ RAD has therefore been selected for development for use in combination with cyclosporine A to prevent acute and chronic rejection after solid organ allotransplantation.

It was first reported in 1989 that the macrolide rapamycin (RPM*), a secondary metabolite of *Streptomyces hygroscopicus*, effectively suppresses the rejection of transplanted allogeneic solid organs in experimental animals (1, 2). RPM is of particular interest as a new immunosuppressant because its mode of action is different from that of both cyclosporine

(CsA) and FK506. The latter drugs prevent T-cell proliferation by blocking transcriptional activation of early T cell-specific genes, thus inhibiting the production of T-cell growth factors, like interleukin (IL)-2. RPM, in contrast, acts at a later stage of the cell cycle, blocking not the production of growth factors but rather the proliferative signal that is provided by these factors; RPM arrests the cells at the late G1 stage of the cell cycle, preventing them from entering the S phase. (For a review on RPM and its mechanism of action see 3, 4). It is of note that this effect of RPM is not restricted to IL-2-driven proliferation of T cells; RPM inhibits growth factor-dependent proliferation in general of any hematopoietic as well as nonhematopoietic cells tested so far (5-7), including vascular smooth muscle cells (VSMC) (8). The different modes of action of RPM and CsA provide a rationale for synergistic interaction of the two compounds, and this synergism has indeed been demonstrated (9-11). Further, the ability to inhibit growth factor-driven cell proliferation makes RPM a potential compound for the prevention of late graft loss due to graft vessel disease (GVD); growth factor-driven proliferation of VSMC leading to intimal thickening and eventually vessel obstruction seems to play a crucial role in the development of GVD (for a review see 12). RPM has indeed been shown to inhibit arterial intimal thickening in rat recipients of orthotopic femoral artery allografts (13) as well as such thickening produced by mechanical injury where no immunological mechanism is involved (14).

These features make RPM and RPM analogs very interesting compounds for clinical transplantation. However, development of a proper oral RPM formulation with acceptable stability, bioavailability, and predictability has proven difficult and has impeded successful clinical development. So far, the majority of published preclinical work demonstrating the potent immunosuppressive effect of RPM deals with paravenous administration of the compound (for references see 15); efficacy of an oral RPM formulation was shown only very recently in a pig and a rat model of allotransplantation (16, 16). However, wide interindividual variation in the pharmacokinetic parameters was noted in the pig study as well as in a recent report on first clinical experience with an oral RPM formulation (17).

The formulation of a compound can have a marked effect on clinical outcomes in transplantation, as seen with the introduction of the microemulsion concentrate of CsA (Neoral; Sandoz, Basel, Switzerland) (18-20). The 40-O-(2-hydroxyethyl)-RPM, SDZ RAD, is a new RPM analog that resulted from our efforts to overcome the formulation problems by chemical derivation, while maintaining the pharmacolog-

¹ Preclinical Research, Novartis Pharma AG.

² Address correspondence to: Walter Schuler, Preclinical Research, Novartis Pharma AG, S-386.1.26, CH-4002 Basel, Switzerland.

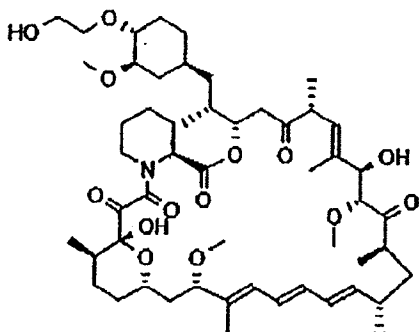
³ Technical Research and Development, Novartis Pharma AG.

* Abbreviations: CsA, cyclosporine; FCS, fetal calf serum; FKBP12, FK506 binding protein; GVD, graft vessel disease; IC₅₀, concentration of compound needed to reach 50% inhibition; IL, interleukin; MLR, mixed lymphocyte reaction; PBMC, peripheral blood mononuclear cells; RPM, rapamycin; VSMC, vascular smooth muscle cells.

July 15, 1997

SCHULER ET AL.

37



SDZ RAD

FIGURE 1. Chemical structure of SDZ RAD, 40-O-(2-hydroxyethyl)-RPM.

ical benefits of RPM. In this study we report on the *in vitro* and *in vivo* pharmacological characteristics of SDZ RAD. We show that despite a slightly reduced *in vitro* activity, SDZ RAD has an efficacy after oral dosing that is at least equivalent to that of RPM.

MATERIALS AND METHODS

Reagents

RPM was obtained by fermentation of the actinomycetes strain A91-258211. SDZ RAD, 40-O-(2-hydroxyethyl)-RPM (Fig. 1), was derived by chemical derivation of RPM; the molecular formula is $C_{67}H_{95}NO_{14}$, and it has a molecular weight of 958.25. For the *in vitro* experiments, 10^{-3} M stock solutions of the compounds in ethanol were used. Stock solutions were stored at -20°C ; samples to be tested were diluted on the day of the experiment in phosphate-buffered saline or culture medium. For the *in vivo* experiments SDZ RAD and RPM were formulated as liquid formulations, which kept the compounds dissolved even after dilution with aqueous vehicles. These formulations were adapted for both compounds with respect to their physicochemical properties. Stored at 4°C , the formulations are stable for >3 months.

In Vitro Assays

The *in vitro* activity of RPM analogs was assessed by determining in the various assays the concentration of the compounds that results in 50% inhibition (IC_{50}). Serial dilutions of the test compounds, done in duplicate, were tested, and a four-parameter logistic function was applied to calculate the IC_{50} values. RPM was included in each individual experiment as a standard, and the inhibitory activity was expressed as relative IC_{50} compared with RPM (i.e., given as the ratio IC_{50} of test compound/ IC_{50} of RPM). To measure *in vitro* cell proliferation, [^3H]thymidine incorporation into DNA was determined following standard procedures.

FKBP12 binding assay. Binding to the FK506 binding protein (FKBP12) was indirectly assessed by means of an ELISA-type competition assay. Microtiter plate wells were coated with FK506 that was covalently coupled to bovine serum albumin. Coupling of FK506 to bovine serum albumin was performed by reacting bovine serum albumin with N-succinimidyl-oxy-carbonyl-S'-propionyl-ox-33-FK506. Biotinylated recombinant human FKBP12 was allowed to bind to the immobilized FK506 in the absence (as a control) and the presence of the serially diluted test compound or standard. (For technical reasons we used FK506 as the standard, as an exception

only in this assay). Bound biotinylated FKBP12 was assessed by incubation with a streptavidin-alkaline phosphatase conjugate, followed by incubation with p-nitrophenol phosphate as a substrate. Readout was the optical density at 405 nm. Binding of a compound to the biotinylated FKBP12 resulted in a decrease in the amount of FKBP12 available for binding to the immobilized FK506, i.e., the magnitude of this inhibition (IC_{50}) reflects the affinity of a compound for FKBP12.

IL-6-driven proliferation of a B-cell hybridoma. The hybridoma B13-29-15 is a subclone of the hybridoma B13-29, which was kindly provided by L. Aarden (Central Laboratory of the Netherlands Red Cross-Blood Transfusion Service, Amsterdam, The Netherlands); this clone is strictly dependent on IL-6. To determine the IC_{50} of a compound in this assay, 10^4 cells per microtiter well (supplemented to contain 0.3 ng of IL-6 per ml) were incubated for 72 hr with serial dilutions of the compounds. [^3H]thymidine was added at the end of the incubation period, 5 hr before harvesting the cells for measuring the [^3H]thymidine incorporation into DNA.

Mixed lymphocyte reaction (MLR). To determine the IC_{50} values of the compounds in a two-way MLR, 10^5 spleen cells per well each of BALB/c and CBA mice were incubated in flat-bottom microtiter plates, either in the absence or the presence of the serially diluted compounds. Serum-free tissue culture medium supplemented with serum replacement factors (CG medium, Camon GmbH, Wiesbaden, Germany) was used. After 4 days of incubation [^3H]thymidine was added, and the cells were harvested after another 16-hr incubation period.

Proliferative response of antigen-specific human T-cell clones. CD4-positive (helper type) T-cell clones specific for the hemagglutinin peptide 307-319 were derived from peripheral blood mononuclear cells (PBMC) of a normal healthy volunteer as described (21). To determine the IC_{50} of the compounds in this antigen-specific T-cell proliferation assay, cloned T cells (2×10^4) were cultured in a total volume of 200 μl of RPMI medium (supplemented to contain 5% human AB serum) in 96-well round-bottom microtiter plates with 10^4 irradiated PBMC from normal HLA-DR matched donors, together with the peptide antigen (hemagglutinin) and the serially diluted test compounds. As a control, T cells plus PBMC in the absence of peptide antigen or T cells in medium alone were included. Cultures were set up in duplicate. After 48 hr of incubation, [^3H]thymidine was added, and the cells were harvested after another 16 hr.

Proliferation of VSMC. Bovine VSMC were derived by the explant technique from small pieces of media (dissected free of adventitia and intima) from fresh bovine aortae. Explants of about 1 mm^3 were placed in culture dishes, covered with medium, and after about 10 days the cells grew out of the explants. The cells were characterized as VSMC by morphology in culture and by immunostaining with an anti-VSMC actin antibody (clone 1A4; Sigma, St. Louis, MO). They were used at passages 2 through 10. The cells were grown in DF10 medium consisting of equal volumes of Dulbecco's modified Eagle's medium and Ham's F12 (Life Technologies, Gaithersburg, MD) supplemented with 10% fetal calf serum (FCS) and glutamine. For the experiments, the cells were seeded in 96-well plates (1×10^4 or 2×10^4 per well) and allowed to grow to confluence (3 days). They were then growth arrested by serum deprivation for 48 hr in serum-free medium (DF10 without FCS) supplemented with insulin (0.5 nM; Boehringer Mannheim, Mannheim, Germany), transferrin (5 $\mu\text{g}/\text{ml}$; Sigma), and ascorbate (0.2 nM; Sigma). After 3 days the medium was replaced with fresh medium containing 10% FCS and [^3H]thymidine (1 mCi/ml), together with serial dilutions of the compounds to be tested (three to four replicate wells for each concentration). The cells were harvested after a 24-hr incubation period and the [^3H]thymidine incorporation into the DNA was measured.

In Vivo Experiments

Throughout all of the *in vivo* experiments the compounds were given once daily, for the indicated period of time. Freshly prepared

CORD078385

A1137

dilutions of the SDZ RAD and RPM formulations with water were given orally by gavage. Control animals received only the administration vehicle as placebo.

Localized graft-versus-host reaction. Spleen cells (2×10^7) from Wistar/F rats were injected subcutaneously into the right hind footpad of (Wistar/F \times Fisher 344) F_1 hybrid rats. The left footpad was left untreated. The animals were treated with SDZ RAD or RPM on 4 consecutive days (days 0–3). The popliteal lymph nodes were removed on day 7, and the weight differences between two corresponding lymph nodes were determined. The results were expressed as the inhibition of lymph node enlargement (given in percent) comparing the lymph node weight differences in the experimental groups to the weight difference between the corresponding lymph nodes from a group of animals left untreated with a test compound.

Mercuric chloride-induced glomerulonephritis. Autoimmune glomerulonephritis was induced by treatment with $HgCl_2$ (22). Female Brown Norway rats, 9 weeks of age, were injected subcutaneously during a 3-week period, three times per week, with 1 mg of $HgCl_2$ per kg body weight (10 injections in total). SDZ RAD and RPM were given on 5 consecutive days per week. On days 0, 7, 14, and 21, urine was taken and the protein concentration was determined by means of bromophenol blue staining and colorimetric detection using a TCL scanner. The detection limit of this method is 1 mg protein/ml; the upper threshold of this method is 16 mg protein/ml. The experiment is normally terminated between day 21 and day 24 because the control animals, treated with $HgCl_2$ only, start to succumb to the disease at this point.

Orthotopic kidney allotransplantation. Donor kidneys were transplanted orthotopically into recipient rats. The left kidney of the recipient animal was removed and replaced with the donor kidney, with end-to-end anastomoses of blood vessels and ureter. After 1 week, contralateral nephrectomy was performed, leaving the animal fully dependent on the grafted kidney. Recipients were treated with the immunosuppressive compounds or the placebo for the initial 2 weeks after transplantation.

Vascular heterotopic heart allotransplantation. Donor hearts were transplanted heterotopically into the abdomen of recipient rats by making end-to-side anastomoses of the donor's aorta with the recipient's infrarenal abdominal aorta as well as with the donor's right pulmonary to the recipient's inferior vena cava. Recipients received the immunosuppressive compounds or the placebo once daily for the entire course of the experiment. The heartbeat of the transplanted heart was monitored daily by palpation of the abdomen. The time of rejection was defined as the day on which a heartbeat was no longer palpable.

RESULTS

Binding to FKBP12

Binding to FKBP12, the abundant intracellular binding protein of FK506, is a prerequisite for the biological activity of RPM-type macrolides (23). Therefore, we determined the ability of SDZ RAD to bind to FKBP12. As shown in Table 1, binding of SDZ RAD to FKBP12 is about threefold weaker than that of RPM.

Inhibition of Growth Factor-Driven Proliferation

The immunosuppressive activity of RPM is explained by its ability to inhibit growth factor-driven cell proliferation. We assessed SDZ RAD for this effect in two *in vitro* systems: IL-6-stimulated cell proliferation of the IL-6-dependent hybridoma clone B13-29-15, and FCS-stimulated proliferation of bovine VSMC. Table 2 shows that the ability of SDZ RAD to inhibit the IL-6-driven proliferation of the hybridoma cells is about two- to threefold less compared with that of RPM (i.e., relative IC_{50} of 2.5 ± 0.7). The relative IC_{50} of SDZ RAD

TABLE 1. Binding to FKBP12^a

Compound	Relative $IC_{50} \pm SD^b$ (range, absolute IC_{50})
FK506	1 (0.8–1.2 nM)
RPM	$0.6 \pm 0.2^*$ (n=5) (0.4–0.9 nM)
SDZ RAD	$2.0 \pm 0.4^{***}$ (n=3) (1.8–2.6 nM)

^a The ability of the compounds to compete with immobilized FK506 for binding to biotinylated FKBP12 was determined in a competitive binding assay.

^b FK506 was included as a standard in each individual experiment. Results are expressed as means \pm SD of the relative IC_{50} values (i.e., ratio of IC_{50} test compound to IC_{50} of FK506). The range of absolute IC_{50} values is given in parenthesis; n=number of individual experiments. Statistical analysis, t test: * $P < 0.05$; *** $P < 0.001$.

TABLE 2. Inhibition of growth factor-stimulated cell proliferation

Compound	Relative $IC_{50} \pm SD^*$ (range, absolute IC_{50})	
	Hybridoma B13-29-15/IL-6	Bovine VSMC/FCS
RPM	1 (0.07–0.5 nM)	1 (0.4–3.5 nM)
SDZ RAD	$2.5 \pm 0.7^{**}$ (n=5) (0.2–1.4 nM)	$1.9 \pm 0.75^{**}$ (n=3) (0.9–3.6 nM)

* RPM was included as a standard in each individual experiment. Results are expressed as means \pm SD of the relative IC_{50} values (i.e., ratio of IC_{50} test compound to IC_{50} of RPM). The range of absolute IC_{50} values is given in parenthesis; n=number of individual experiments. Statistical analysis, t test: ** $P < 0.01$; ***not significant.

for inhibition of bovine VSMC was 1.9 ± 0.75 (Table 2); however, this was not statistically significant when compared with inhibition by RPM. The absolute IC_{50} values found here for RPM are in agreement with those reported for platelet-derived growth factor or basic fibroblast growth factor-stimulated VSMC proliferation (5 nM and 0.8 nM, respectively (8)).

Immunosuppressive Activity *In Vitro*

The immunosuppressive activity of SDZ RAD was assessed in two-way MLR experiments with lymphocytes of mouse origin as well as in experiments with antigen-specific human helper T-cell clones. The results are shown in Table 3. The data show that, compared with RPM, the *in vitro* immunosuppressive activity of SDZ RAD is about two- and fivefold lower, respectively, in these assays.

TABLE 3. Immunosuppressive activity *in vitro*^a

Compound	Relative $IC_{50} \pm SD^b$ (range, absolute IC_{50})	
	MLR	T-cell clone
RPM	1 (0.06–0.9 nM)	1 (0.014–0.037 nM)
SDZ RAD	$2.1 \pm 0.4^*$ (n=4) (0.2–1.6 nM)	$5.4 \pm 3.5^*$ (n=3) (0.05–0.17 nM)

^a The effect on two-way MLR performed with mouse spleen cells, as well as on the antigen-specific (hemagglutinin peptide 307–319) proliferation of a human T-cell clone, was tested.

^b As in Table 2. Statistical analysis, t test: * $P < 0.05$.

July 15, 1997

SCHULER ET AL.

39

Inhibition of Localized Graft-Versus-Host Reaction

In this experimental model of cell-mediated immunity, a strong local T-cell reaction is induced by injecting parental spleen cells into one hind footpad of F_1 hybrid recipients. The injected immunocompetent donor spleen cells home to the local draining popliteal lymph node, where they react vigorously to alloantigens present on the host's cells; they become activated, secrete cytokines, and proliferate. This reaction manifests itself in an enlargement of the respective lymph node. Comparing the weight of the popliteal lymph node from the site of injection with that of the untreated contralateral lymph node gives an indication of the severity of the reaction. SDZ RAD effectively inhibited lymph node swelling elicited by this localized graft-versus-host reaction. This is shown in Table 4. Maximal inhibition of about 70–80% was achieved with an oral dose of 3 mg/kg per day of either SDZ RAD or RPM. (Increasing the doses of SDZ RAD or RPM did not lead to stronger inhibition of lymph node swelling; data not shown). Inhibition was statistically significant with respect to the placebo-treated control; no statistically significant difference was found between SDZ RAD and RPM.

Mercuric chloride-induced glomerulonephritis. Low doses of mercuric chloride ($HgCl_2$), repeatedly injected into rats, induce an autoimmune disease that is characterized by a T-dependent polyclonal B-cell activation (22, 24). This polyclonal B-cell activation leads to the production of a variety of autoantibodies. Antibodies directed against the glomerular basement membrane cause infiltration of polymorphonuclear granulocytes and glomerular damage; the animals develop a severe proteinuria within 2 to 3 weeks of treatment with $HgCl_2$. As can be seen from Table 5, a dose of 1.25 mg/kg/day of SDZ RAD or RPM completely prevented this $HgCl_2$ -induced development of proteinuria. (One animal in the RPM group showed proteinuria already on day 7, but this was most likely not related to the $HgCl_2$ treatment). The 0.3 mg/kg dose was ineffective, whereas 0.6 mg/kg of either compound led to partial inhibition. In conclusion, SDZ RAD is effective in an animal model for autoimmune glomerulonephritis, with the same dose-response relationship as RPM.

Orthotopic Kidney Allotransplantation in the Rat

SDZ RAD was tested in rat kidney allotransplantation using several donor-recipient strain combinations. Grafted recipients underwent contralateral nephrectomy 7 days after transplantation so that the survival of an animal depended fully on the function of the grafted allogeneic kidney. A peculiarity of this rat model is that a 2-week treatment with

TABLE 4. Inhibition of localized graft-versus-host reaction

Compound	No. of animals ^b	Percent inhibition of lymph node swelling ^a	
		1.0 mg/kg/day p.o.	3.0 mg/kg/day p.o.
SDZ RAD	5	58 ± 23**	77 ± 9***
RPM	5	61 ± 22**	66 ± 11***

^a Lymph node weight differences were determined on day 7. Results are given as mean values ± SD of inhibition compared with a control group of five animals that received the vehicle only. The weight differences between the respective lymph nodes from animals in the control group was 34 ± 2 mg. Statistical analysis (analysis of variance) with respect to the control group: ** $P < 0.01$; *** $P < 0.001$.

^b Number of animals in each dosage group.

TABLE 5. Mercuric chloride-induced glomerulonephritis

Compound	Development of proteinuria			
	Vehicle	0.3 mg/kg p.o.	0.6 mg/kg p.o.	1.25 mg/kg p.o.
Control	10/10 ^a			
SDZ RAD		8/9	7/11**	0/9***
RPM		5/5	2/5**	1/5**

^a Number of animals on day 21 with proteinuria (i.e., urine protein levels > 2 mg/ml) of total number of animals in each dosage group. Statistical analysis (chi-square) with respect to control: ** $P < 0.01$; *** $P < 0.001$.

CaA results in the indefinite survival of the graft, a phenomenon that is restricted to rats and is not seen with any other species.

Table 6 shows the results for SDZ RAD and RPM in experiments transplanting kidneys from (Wistar/F × Fisher 344)F₁ donors into Wistar/F recipients. Untreated control animals showed severe cellular rejection on day 7. In this strain combination, donor and recipient are partly matched; prolonged graft survival can thus be obtained with rather low levels of immunosuppression. Survival times of more than 100 days were obtained with 0.5 mg/kg of either SDZ RAD or RPM. At this dose no histological signs of rejection were seen with SDZ RAD, whereas one animal in the RPM group showed moderate signs of chronic rejection. A dose of 0.25 mg/kg SDZ RAD led to a substantial prolongation of the graft survival time in three of nine recipients; no histological signs of rejection were found in these long-term survivors.

The results of kidney allograft experiments using a strain combination with a strong mismatch, i.e., Brown Norway rat donor and Lewis rat recipient, are shown in Table 7. Untreated control animals showed severe cellular rejection on day 7. A dose of 2.5 mg/kg of either SDZ RAD or RPM prolonged the survival of Brown Norway kidneys in most of the Lewis recipients for more than 80 days. The long-term survivors in the SDZ RAD group showed marginal signs of chronic rejection. Even with 1 mg/kg, substantial prolongation of graft survival times was achieved, with one animal in the SDZ RAD group not rejecting its graft during the observation period (78 days). This animal showed histologically moderate chronic rejection. The other animals in this group showed moderate to severe cellular rejection, whereas all animals in the respective RPM group showed severe cellular rejection.

Vascular Heterotopic Heart Allotransplantation

SDZ RAD was further tested in the model of vascular heterotopic heart allotransplantation in the rat using DA rats as donors and Lewis rats as recipients. This strain combination represents a very strong mismatch and is considered the most stringent rat transplantation model. As Table 8 shows, we were unable to achieve long-term graft survival with any dose of SDZ RAD or RPM tested, even though we treated the animals daily until rejection occurred. Increasing the dose from 2.5 to 5 mg/kg of either compound did not improve graft survival times; rather, the higher doses led to severe weight loss under these conditions, forcing termination of the experiments 3 to 4 weeks after transplantation. Only moderate signs of rejection were found histologically in all groups, with the exception of the 1 mg/kg SDZ RAD group, in which rejection was severe. Although we did

CORD078387

TABLE 6. Suppression of allograft rejection of (Wistar/F \times Fisher344)F₁ rat donor kidneys in Wistar/F recipients^a

Compound	Individual survival times (days after transplantation) after treatment		
	0.25 mg/kg/day	0.5 mg/kg/day	1.0 mg/kg/day
SDZ RAD	7, 7, 7, 7, 7, ≥ 61 , ≥ 100 , ≥ 100 ^b	≥ 100 , ≥ 100 , ≥ 100 , ≥ 100 , ≥ 100	≥ 100 , ≥ 100 , ≥ 100
RPM	7, 7, 7, 7, 7, 12	7, ≥ 100 , ≥ 100 , ≥ 100 , ≥ 100	≥ 100 , ≥ 100 , ≥ 100

^a The immunosuppressive compounds were administered p.o. daily from day 0 through day 13 at the indicated dose. Placebo-treated animals showed severe cellular rejection by day 7.

^b Each figure indicates the survival time after transplantation of an individual animal. More than or equal to sign (\geq) indicates that the animal was killed for histology while the animal was in good health and the graft was still functioning.

TABLE 7. Suppression of allograft rejection of Brown Norway rat donor kidneys in Lewis recipients

Compound	Individual survival times (days after transplantation) after treatment	
	1.0 mg/kg/day p.o.	2.5 mg/kg/day p.o.
SDZ RAD	20, 20, 26, 37, ≥ 78 ^a	26, ≥ 80 , ≥ 100 , ≥ 100 , ≥ 100
RPM	18, 22, 26	35, ≥ 83 , ≥ 83

^a As in Table 6.

TABLE 8. Prolongation of DA rat heart allograft survival in Lewis rat recipients^a

Compound	Individual survival times (days after transplantation) after treatment		
	1.0 mg/kg/day	2.5 mg/kg/day	5.0 mg/kg/day
SDZ RAD	12, 14, 14 ^a	18, 22, 26, 27, ≥ 28	22, 33
RPM	12, 15, 27	25, 31, 33, ≥ 81	22, 32

^a The immunosuppressive compounds were administered p.o. daily continuously throughout the entire experiment. Placebo-treated animals showed severe cellular rejection between day 7 and 10.

^b As in Table 6.

not achieve long-term survival in this strain combination with SDZ RAD or RPM given alone, we did with a combination of low doses of SDZ RAD and CaA, indicating synergy of the two compounds (25).

DISCUSSION

The immunosuppressant SDZ RAD is a novel RPM derivative in which the hydroxyl at position 40 of RPM has been alkylated with a 2-hydroxyethyl group. The introduction of this functionalized side chain results in altered physicochemical properties with respect to RPM, i.e., the solubility in several organic solvents and galenic excipients is markedly increased. Several C40-modified analogs of RPM, like esters, carbonates, and carbamates have been previously described in the patent literature. These derivatives can be viewed as prodrugs of RPM, as the newly introduced functional groups are known to be susceptible to hydrolytic cleavage under physiological conditions. The strategy we pursued was aimed at modifications that are resistant to hydrolytic and metabolic degradation. Therefore a series of 40-O-alkylated RPM analogs was prepared (26), of which the 40-O-hydroxyethyl-derivative, SDZ RAD, proved to be the most active representative, both in vitro and in vivo. SDZ RAD binds with high affinity to FKBP12, which is a prerequisite for the inhibitory activity of immunosuppressants belonging to the RPM class (23). The binding of SDZ RAD to FKBP12 is about threefold weaker than that of RPM. This rather small loss of affinity can be attributed to the fact that C40-O-alkylation disrupts

the hydrogen bond existing in the FKBP12/RPM complex between the C40 hydroxyl and the Gln-53 main chain carbonyl (27, 28). Steric interaction between the hydroxyethyl side chain of SDZ RAD and FKBP12 might also contribute to the slightly reduced binding. SDZ RAD has the same mode of action as RPM. At the molecular level SDZ RAD blocks, as RPM, activation of p70 S6 kinase (Schuler, unpublished results); blocking the activation of this kinase is one of the discussed explanations for the growth-inhibitory effect(s) of RPM (4). Further, like RPM, SDZ RAD at subnanomolar concentrations inhibits growth factor-driven cell proliferation, like that of a B-cell hybridoma or that of VSMC. Likewise, it inhibits mouse MLR and antigen-driven proliferation of antigen-specific human T-cell clones. In general, the in vitro activity of SDZ RAD is about two to three times lower when compared with RPM. The degree to which the in vitro activity is reduced is consistent with the observed decrease of affinity for FKBP12 and the demonstrated requirement of FKBP12 binding for immunosuppressive activity (23, 29).

When administered orally at doses between 1 mg/kg/day and 5 mg/kg/day, SDZ RAD is effective in relevant animal models comprising an autoimmune disease model and several allotransplantation models. It should be emphasized that it is impossible to compare directly our results obtained with SDZ RAD with results published by others on the in vivo efficacy of RPM because different galenical formulations and, in most cases, only parenteral administration routes were used in the studies reported in the literature. We therefore compared the oral activity of the two compounds by using our own galenical formulation of RPM, which was developed following the same principle as for SDZ RAD. These formulations were adapted for both compounds with respect to their physicochemical properties. Using this type of formulation, we have shown that SDZ RAD in vivo is at least equipotent to RPM when given orally. This is in contrast to the lower in vitro activity of SDZ RAD. This observed difference between the relative in vitro and the relative in vivo activity cannot simply be explained by differences in the exposure to the two compounds: treatment with the same doses of our RPM and SDZ RAD formulations led to comparable exposure to the two compounds. Daily treatment with 1.5, 5, and 15 mg/kg SDZ RAD resulted in area under the concentration-time curve values on day 28 of 435, 1468, and 6076 ng·h/ml, respectively. The same treatment with RPM led to area under the concentration-time curve values of 228, 1104, and 4071 ng·h/ml, respectively. Also, formation of RPM or pharmacologically active RPM metabolites cannot serve as a possible explanation. Any biotransformation pathway leading to the formation of RPM or its metabolites would require the cleavage of the hydroxyethyl side-chain by initial hydroxylation. From metabolism studies in vitro, as well as in animals,

July 15, 1997

SCHULER ET AL.

41

we do not have evidence that this happens to any significant degree, i.e., SDZ RAD is not a prodrug of RPM. Rather, we suggest as an explanation that the chemical modification in SDZ RAD, which altered its physicochemical properties, led to more favorable pharmacokinetic properties (e.g., disposition of compound), which compensate in vivo for the observed lower in vitro activity. Considering the relatively narrow therapeutic window of these drugs, more favorable pharmacokinetic properties promise to provide a clinical advantage, i.e., it should be easier to handle and to monitor such a drug in clinical practice.

Finally, a major unsolved problem in clinical allotransplantation is long-term graft loss due to chronic rejection. The pathogenesis of chronic rejection is complex and multifactorial in nature. A major factor contributing to late graft loss is intimal thickening of the graft vessels, which eventually leads to vessel occlusion (GVD). Intimal thickening is due to growth factor-driven proliferation and migration of VSMC after injury of the endothelium (for a review see 12). Clinical observations have shown a close correlation between the frequency as well as the intensity of acute rejection episodes and the incidence of chronic rejection (30-33). It can thus be inferred that one triggering event that eventually leads to chronic rejection is an alloimmune injury of the graft vessels. On the other hand, vascular damage resulting from nonimmunological events, e.g., from ischemia or reperfusion injury, also can lead to intimal thickening and may contribute to late graft loss (12). Taking these considerations into account, a two-pronged approach seems most promising for improving the long-term prospects in allotransplantation. This approach would provide improved immunosuppression, to prevent an alloimmune insult in the first place, combined with measures to prevent VSMC proliferation and/or migration. With respect to the first consideration, we have shown here that SDZ RAD efficiently prevents allograft rejection in the rat; in an accompanying publication (25) we report that in animal models for allotransplantation, SDZ RAD and CsA act in a synergistic manner. This synergism, if proven in humans, offers the chance to increase the efficacy of the immunosuppressive regimen by combining the two drugs, with the prospect of mitigating their respective side effects. We have further shown here that SDZ RAD efficiently inhibits the growth factor-stimulated in vitro proliferation of VSMC cells. Elsewhere we will report (H. Schuurman et al., manuscript in preparation) that SDZ RAD also inhibits in vivo vascular changes that were induced either by mechanical damage (balloon catheter injury) or by an alloimmune reaction (aorta transplantation in an allogeneic setting). We believe that the increased immunosuppressive efficacy of a drug combination composed of CsA and SDZ RAD, combined with the ability of SDZ RAD to inhibit VSMC proliferation, bears the potential for improving the prospects for long-term graft acceptance.

Acknowledgments. The authors thank Dr. J. Borel for critical review of the manuscript and comments, and Y. Hartmann, H. Jundt, J. Joergensen, T. Meerloo, U. Strittmatter, M. Tanner, B. Thai, C. Wilt, and C. Witslaand for their expert technical assistance.

REFERENCES

1. Calne RY, Collier DS, Lim S, et al. Rapamycin for immunosuppression in organ allografting. *Lancet* 1989; 2: 227.
2. Morris RE, Meiser BM. Identification of a new pharmacologic action for an old compound. *Med Sci Res* 1989; 17: 609.
3. Morris RE. Rapamycin: antifungal, antitumor, antiproliferative, and immunosuppressive macrolides. *Transplant Rev* 1992; 6: 39.
4. Sehgal SN. Rapamune (sirolimus, rapamycin): an overview and mechanism of action. *Ther Drug Monit* 1996; 17: 660.
5. Hatfield SM, Mynderse JS, Roehm NW. Rapamycin and FK506 differentially inhibit mast cell cytokine production and cytokine-induced proliferation and act as reciprocal antagonists. *J Pharmacol Exp Ther* 1992; 261: 970.
6. Hultsch T, Martin R, Hohman RJ. The effects of the immunophilin ligands rapamycin and FK506 on proliferation of mast cells and other hematopoietic cell lines. *Mol Biol Cell* 1992; 3: 981.
7. Akselband Y, Harding MW, Nelson PA. Rapamycin inhibits spontaneous and fibroblast growth factor β -stimulated proliferation of endothelial cells and fibroblasts. *Transplant Proc* 1991; 23: 2833.
8. Cao W, Mohacsi P, Shorthouse R, Pratt R, Morris RE. Effects of rapamycin on growth factor-stimulated vascular smooth muscle cell DNA synthesis. *Transplantation* 1995; 59: 390.
9. Morris RE, Meiser BM, Wu J, Shorthouse R, Wang J. Use of rapamycin for suppression of alloimmune reactions in vivo: schedule dependence, tolerance induction, synergy with cyclosporine and FK506, and effect on host-versus-graft and graft-versus-host reactions. *Transplant Proc* 1991; 23: 621.
10. Tu Y, Stepkowski SM, Chou T-C, Kahan BD. The synergistic effects of cyclosporine, sirolimus, and brequinar on heart allograft survival in mice. *Transplantation* 1995; 59: 177.
11. Martin DF, DeBargo LR, Nussensblatt RJ, Chan CC, Roberge FG. Synergistic effect of rapamycin and cyclosporin A in the treatment of experimental autoimmune uveoretinitis. *J Immunol* 1996; 154: 922.
12. Hayry P, Isoniemi H, Yilmaz S, et al. Chronic allograft rejection. *Immunol Rev* 1993; 134: 39.
13. Gregory CB, Huie P, Billingham ME, Morris RE. Rapamycin inhibits arterial intimal thickening caused by both alloimmune and mechanical injury. *Transplantation* 1993; 55: 1409.
14. Gregory CB, Huang X, Pratt RE, et al. Treatment with rapamycin and mycophenolic acid reduces arterial intimal thickening produced by mechanical injury and allows endothelial replacement. *Transplantation* 1995; 59: 655.
15. Granger DK, Cromwell JW, Chen SC, et al. Prolongation of renal allograft survival in a large animal model by oral rapamycin monotherapy. *Transplantation* 1995; 59: 183.
16. DiJoseph JF, Fuhler E, Armsrong J, Sharr M, Sehgal SN. Therapeutic blood levels of sirolimus (rapamycin) in the allografted rat. *Transplantation* 1996; 62: 1109.
17. Kahan BD, Murgia MG, Slaton J, Napoli K. Potential applications of therapeutic drug monitoring of sirolimus immunosuppression in clinical renal transplantation. *Ther Drug Monit* 1996; 17: 672.
18. Kovarik JM, Mueller EA, van Bree JB, et al. Cyclosporine pharmacokinetics and variability from a microemulsion formulation: multicenter investigation in kidney transplant patients. *Transplantation* 1994; 58: 1.
19. Taesch S, Niese D. Safety and tolerability of a new oral formulation of cyclosporin A, Sandimmun Neoral, in renal transplant patients. *Transpl Int* 1994; 7(suppl 1): 263.
20. Mueller EA, Kovarik JM, van Bree JB, Lison AE, Kutz K. Safety and steady-state pharmacokinetics of a new oral formulation of cyclosporin A in renal transplant patients. *Transpl Int* 1994; 7(suppl 1): 267.
21. Lamb JR, Eckels DD, Lake P, Woody JN, Green N. Human T cell clones recognize chemically synthesized peptides of influenza haemagglutinin. *Nature* 1982; 300: 66.
22. Hirsch F, Coudere J, Sapin C, Fournié G, Druet P. Polyclonal effect of HgCl₂ in the rat: its possible role in an experimental

CORD078389

A1141

- autoimmune disease. *Eur J Immunol* 1982; 12: 620.
22. Dumont FJ, Melino MR, Staruch MJ, Koprak SL, Fischer PA, Sigal NH. The immunosuppressive macrolides FK506 and rapamycin act as reciprocal antagonists in murine T cells. *J Immunol* 1990; 144: 1418.
 24. Druet P, Palletier L, Rossert J, Druet E, Hirsch F, Sapin C. Autoimmune reactions induced by metals. In: Kammüller ME, Bloksma N, Seinen W, eds. Autoimmunity and toxicology: immune dysregulation induced by drugs and chemicals. Amsterdam: Elsevier Science Publishers, 1989: 347.
 25. Schuurman HJ, Cottens S, Fuchs S, et al. SDZ RAD, a new rapamycin derivative: synergism with cyclosporine. *Transplantation* 1997; 64: 32.
 26. Cottens S, Sedrani R. O-Alkylated rapamycin derivatives and their use, particularly as immunosuppressants. PCT International patent application 1994; WO 94/09010-A1. [Chem Abstr 1994; 122: 9774a].
 27. Van Duyn JD, Standaert RF, Schreiber SL, Clardy J. Atomic structure of the rapamycin human immunophilin FKBP-12 complex. *J Am Chem Soc* 1991; 113: 7423.
 28. Van Duyn JD, Standaert RF, Karplus PA, Schreiber SL, Clardy J. Atomic structures of the human immunophilin FKBP-12 complexes with FK506 and rapamycin. *J Mol Biol* 1993; 229: 105.
 29. Cottens S, Fehr T, Quesniaux V, Schuler W, Sedrani R, Zanke G. The role of immunophilin binding in the immunosuppressive properties of CaA, FK506 and rapamycin derivatives. *Acta Chim Ther* 1994; 21: 83.
 30. Gulanikar AC, MacDonald AS, Sungurtekin U, Balitsky P. The incidence and impact of early rejection episodes on graft outcome in recipients of first cadaver kidney transplants. *Transplantation* 1992; 53: 323.
 31. Basadonna GP, Matas AJ, Gillingham KJ, et al. Relationship between early vs late acute rejection and onset of chronic rejection in kidney transplantation. *Transplant Proc* 1993; 25: 910.
 32. Matas AJ, Gillingham KJ, Payne WD, Najarian JS. The impact of an acute rejection episode on long-term renal allograft survival ($t_{1/2}$). *Transplantation* 1994; 57: 876.
 33. Pirsch JD, Ploeg RJ, Gange S, et al. Determinants of graft survival after renal transplantation. *Transplantation* 1996; 61: 1581.

Received 18 August 1996.

Accepted 4 April 1997.

0043-1337/97/0401-42\$03.00/0

TRANSPLANTATION

Copyright © 1997 by Williams & Wilkins

Vol. 64, 42-48, No. 1, July 15, 1997

Printed in U.S.A.

MECHANISM OF CONCORDANT CORNEAL XENOGRAFT REJECTION IN MICE

SYNERGISTIC EFFECTS OF ANTI-LEUKOCYTE FUNCTION-ASSOCIATED ANTIGEN-1 MONOCLONAL ANTIBODY AND FK506^{1,2}

SATORU YAMAGAMI,^{3,4,5} MITSUAKI ISOBE,⁶ HIROKO YAMAGAMI,⁷ JUNKO HORI,⁴ AND TADAHIKO TSURU⁴

Department of Ophthalmology, Jichi Medical School, Kawachi-gun, Tochigi; Department of Ophthalmology, University of Tokyo School of Medicine, Bunkyo-ku, Tokyo; First Department of Internal Medicine, Shinshu University School of Medicine, Matsumoto, Nagano; and Department of Ophthalmology, Tokyo Women's Medical College, Shinjuku-ku, Tokyo, Japan

Background. The mechanisms of corneal xenogeneic immunoreaction, as well as the potential role of immunosuppressive therapy in the suppression of corneal xenograft rejection, have not been thoroughly explored.

¹ This work was supported by grants H06454495 and A08771519 from the Scientific Research Department of the Ministry of Education, Science, and Culture of Japan and by a grant from the Japan National Society for the Prevention of Blindness.

² Presented in part at the annual meeting of the Association for Research in Vision and Ophthalmology, Fort Lauderdale, FL, April 24, 1996.

³ Department of Ophthalmology, Jichi Medical School.

⁴ Department of Ophthalmology, University of Tokyo School of Medicine.

⁵ Address correspondence to: Satoru Yamagami, MD, Department of Ophthalmology, Jichi Medical School, 3311-1 Yakushiji, Minamikawachi, Kawachi-gun, Tochigi 329-04, Japan.

⁶ First Department of Internal Medicine, Shinshu University School of Medicine.

⁷ Department of Ophthalmology, Tokyo Women's Medical College.

Methods. BALB/c mice who received orthotopic corneal transplants (Lewis rats donors) were administered intraperitoneally anti-leukocyte function associated antigen-1 (LFA-1) monoclonal antibody (mAb) or FK506 (3 mg/kg/day) or both of these immunosuppressants during a 12-day postoperative period. Histological (hematoxylin-eosin stain) and immunohistochemical evaluations of enucleated eyes were performed. Humoral immune response and delayed-type hypersensitivity (ear-swelling assay) were evaluated.

Results. The mean (\pm SD) graft survival time in the untreated control, FK506-treated, anti-LFA-1 mAb-treated, and combined-treatment groups was 5.3 ± 0.8 , 9.4 ± 4.0 , 8.7 ± 5.0 , and 67.7 ± 18.4 days, respectively. In the untreated control group, mouse IgG, IgM, and C3 were expressed on the rat corneal grafts during the early postoperative phase. Flow cytometry studies revealed high titers of xenoreactive IgG and IgM antibodies. T helper 1 cytokines were expressed on xenografted corneal beds, and delayed-type hypersen-

CORD078390

